



---

# Decarbonization of the electricity, heating, and transport sectors on Samsø

Master Thesis Project  
Spring 2021

---

Author:

Tilde Lyngsø, au519382

Supervisors:

Marta Victoria,.mvp@eng.au.dk

Gorm Bruun Andresen, gba@eng.au.dk



AARHUS  
UNIVERSITY  
DEPARTMENT OF ENGINEERING

## ABSTRACT

---

In 1997 Samsø was named the renewable energy island of Denmark, and it has lived up to that name, achieving carbon neutrality in just ten years. This was done by installing wind turbines and receiving extra CO<sub>2</sub>-quotas from the export of 70% of the island's renewable electricity generation to the mainland. In 2007 the island opened an Energy Academy dedicated to energy savings and the transition to renewable energy, continuing to set new goals for the island after it met the initial targets.

The next goal the island has set for itself is to become completely independent of fossil fuels. A necessary step if the island wishes to stay carbon-neutral without the extra CO<sub>2</sub> quotas, which will stop in 2030 when the Danish electricity sector is expected to become carbon neutral. Currently, the island's need for fossil fuels is practically limited to the transport sector and a significant part of the private heating demand. Removing fossil fuels from private the heating sector requires persuading the residents to replace the remaining oil burners. While this is not an easy task, a wide range of alternative heating sources make it seem like a simple project compared to the transport sector, which more challenges.

With the share of electric cars in the private transport sector slowly increasing on its own, the main task is to find a way to meet the demand for heavy transport like ferries, tractors, and trucks without relying on fossil fuels. Constructing a biogas plant on the island could be part of the solution to this problem. However, this would lay claim to some of the local biomass, which is currently being used to fuel the district heating sector. As the island wishes to avoid depending on the biomass import for the biogas plant, it is relevant to explore alternative heat sources for the district heating sector. An obvious choice is large-scale heat pumps, a CO<sub>2</sub>-neutral option, as long as renewable sources generate the electricity.

In this thesis, a technical-economic analysis is performed to determine if the electrification of the district heating sector is cost-competitive with the current biomass burners. The operation of the electrified district heating plant is examined in detail, and it is investigated how sensitive the optimal capacities are to external factors, such as annual variations, component costs, and varying electricity cost. With the electrification of the heat and transport sector, the electricity demand on the island will increase. To examine how this increase in demand affects the energy

system on Samsø, the energy generation and consumption on the island is modelled as a "Smart Energy System". Here, the coupling between the electricity, heat and transport sectors allows the system to balance the production and demand in all three sectors by using the storage in the transport and district heating sector. The inclusion of the connection to Jutland in the model allows the island to import electricity when necessary and to export electricity to the mainland when production exceeds local demand.

In this project, the following questions are examined:

*Is the production cost for an electrified district heating plant cost-competitive with biomass burners?*

*What are the effects of increasing synergy between the energy sectors on Samsø?*

*Can Samsø benefit from increasing its renewable capacities?*

All systems are modelled for a full year in hourly snapshots, and an optimisation algorithm is applied to determine the capacities and operation, which result in the lowest system cost while meeting the required demands every hour.

When optimising the district heating plant in Ballen-Brundby for an air-sourced heat pump, the plant's electrification results in a direct heat production cost equal to the current cost of 35 €/MWh. With a ground-sourced heat pump, the production cost is slightly lower at 33 €/MWh, but this solution has a higher investment cost. The lowest overall system cost is therefore found when using an air-sourced heat pump. When the district heating plant is based on an air-sourced heat pump, the recommended configuration consists of a heat pump of 1.2 MW<sub>thermal</sub>, along with a resistive heater of 1.0 MW. The resistive heater functions to cover the peak load in the colder months to reduce the capacity of the expensive heat pump. The system also includes heat storage of 21 MWh, which mainly functions to balance the electricity cost, allowing the system to increase the heat production when the electricity price is low and discharge the storage in the morning and evening when the electricity price is high.

A coupling of the energy sectors on Samsø results in a decrease in electricity export as the annual electricity demand on the island increases. The conversion to an electrified district heating sector also increases the annual system cost, as the expense of the capital and marginal costs associated with the district heating sector are now included. When the transport sector is included, the island residents cover the associated capital costs, but the system covers the increase in electricity demand. However, the system also gets the advantage of using the batteries in the electric vehicles to store electricity, which can later be discharged into the grid. This advantage reduces the annual system cost by an average of 2%, as the system is allowed to import electricity when the spot price is low and sell it at a profit later.

When looking at the energy system for Samsø, the renewable resource quality is higher than the Danish average. However, despite the higher than average wind quality, the installation of more wind is not cost-competitive with the current electricity market, even as the cost of wind turbines decreases towards 2050. The same cannot be said for solar PV, where the current cost is on the verge of making solar panels cost-optimal. This is revealed by the fact that the capital cost of solar is too high to warrant an increase in solar panels for a year with an average amount of sunny hours. However, it is cost-optimal to increase the solar panels on Samsø by 45 MW for a slightly above average year. The same is seen when the associated cost decrease in the future, where the expected cost in 2030 makes it cost-optimal to increase the islands solar panels by 55 MW.

The reduction in installation costs associated with renewable energy makes it beneficial for the island to increase the link capacity to the mainland by 2040. In both 2040 and 2050, the increase in link capacity is 10 MW or 25%, allowing the system to install the maximum permitted solar capacity of 81.3 MW. Nevertheless, reaching the limit for solar panels does not result in an increase in on- or offshore wind turbines unless the cost of wind turbines is reduced significantly beyond expected values.

## ACKNOWLEDGEMENTS

---

First and foremost, I would like to thank Marta Victoria for supervising my project. Her expertise, guidance, and encouragement has helped greatly both in defining and completing this project. Additionally, her kindness and unwavering support have always left me with renewed confidence in both myself and this project after our meetings, even during my biggest crises.

I would also like to thank Gorm Bruun Andresen for his input and guidance during the project. Having an extra person to review my work and progress has been immensely helpful.

I extend my gratitude towards Jan Jantzen for inspiring the project, helping to guide me through it and providing data. Even though it wasn't possible to work on the project on Samsø, working on a project related to the island has felt like coming home.

Furthermore, I would like to thank Line Harfeld Møller for our writing fellowship; without the structure it helped provide, it would have been difficult for me to complete this project. While this fellowship has allowed for academic discussions and a readily available source of input when needed, I am most grateful for her support, humour and the friendship, which has developed over the course of this project.

Finally, I would like to thank Victor Matchkov and the people who have guested Lines and my private Friday Bar. At the end of a long week, they have helped switch the focus from renewable energy solutions to alcoholic ones.

## NOMENCLATURE

---

*BBDH* Ballen-Brundby district heating plant

*BEV* Battery Electric Vehicle

*COP* Coefficient of Performance

*DH* District Heating

*DK1* Jutland and Funen

*HDH* Heating Degree Hours

*HGL* Hourly Grid Loss

*HP* Heat Pump

*HWD* Hourly hot Water Demand

*ICE* Internal Combustion Vehicles

*PV* Photovoltaic

*RH* Resistive Heater

*SHD* Space Heating Demand

*VRES* Variable Renewable Energy Sources

# CONTENTS

---

<b>1</b>	<b>Introduction</b>	<b>1</b>
1.1	The island of Samsø . . . . .	1
1.2	Renewable Energy Island . . . . .	2
1.3	Project outline . . . . .	3
<b>2</b>	<b>Methods</b>	<b>5</b>
2.1	Assumptions . . . . .	5
2.2	Python for Power System Analysis . . . . .	6
2.3	Electricity . . . . .	7
2.4	Heating . . . . .	11
2.5	Hydrogen . . . . .	21
2.6	Transport . . . . .	22
<b>3</b>	<b>Ballen-Brundby District heating plant</b>	<b>26</b>
3.1	Initial results . . . . .	26
3.2	Sensitivity analysis . . . . .	29
3.3	Recommended system and cost analysis . . . . .	35
3.4	Discussion . . . . .	36
<b>4</b>	<b>Samsø energy system</b>	<b>38</b>
4.1	Current VRES capacities . . . . .	39
4.2	Expanding VRES capacities . . . . .	44
4.3	Discussion . . . . .	53
<b>5</b>	<b>Conclusion</b>	<b>55</b>
<b>A</b>	<b>Individual Heat demand</b>	<b>63</b>
A.1	Heat pump COP . . . . .	64
<b>B</b>	<b>Scaling of time series data</b>	<b>65</b>

b.1	Wind capacity factors . . . . .	65
b.2	Electricity demands . . . . .	66
<b>C</b>	<b>Model overviews</b>	<b>67</b>

## LIST OF FIGURES

---

Figure 1	Overview of installed and proposed infrastructure in the energy sector on Samsø. . . . .	2
Figure 2	Cost optimisation in PyPSA. . . . .	6
Figure 3	Overview of the current electricity system on Samsø. . . . .	8
Figure 4	System model for BBDH. Capacity and dispatch are optimised for the components marked in bold. . . . .	11
Figure 5	Comparison between measured and modelled temperatures. . . . .	15
Figure 6	$\chi^2$ -distribution for 11 degrees of freedom and critical values. . . . .	16
Figure 7	Comparison between historic and modelled heat production for the highest and lowest $\chi^2$ values for a threshold temperature of 16°C. . . . .	17
Figure 8	Hourly heat production for each category for 2018. . . . .	18
Figure 9	COP for the air- and ground-sourced heat pumps in 2018. The actual COP is considerably higher than the nameplate COP for most of the year.	20
Figure 10	Historical measured temperature on Samsø. . . . .	21
Figure 11	Model overview for hydrogen storage. The components, which are optimised, are marked in bold. . . . .	22
Figure 12	Model overview for transport sector. . . . .	23
Figure 13	Daily profile for the transport demand. When the vehicle is not in use, it is assumed to be connected to the grid. All connected cars are available for charge, 25% are also available for discharge. . . . .	24
Figure 14	Flowchart for the analysis of Ballen-Brundby district heating plant. . . . .	26
Figure 15	Heat production, electricity price, and charging, discharging and filling level for heat storage throughout the year in 2018. . . . .	27
Figure 16	Ramps for heat pump and resistive heater the years 2013-2019. . . . .	28
Figure 17	Average daily heat production by source and required heat output in 2018. Storage is used to balance mismatch between heat production and the required output. . . . .	28
Figure 18	Duration curves and average daily heat production for BBDH in 2018. . . . .	29

Figure 19	Sensitivity to cost variations based on values for 2018. To provide a scale for the different cost variations and their impact on the capacities and the annual system cost, the grid lines in all figures have a distance of 20%. The initial values can be seen in the legend. . . . .	30
Figure 20	Comparison of heat pump production with a ramping limit of 0.10 and without ramping limit. . . . .	31
Figure 21	Sensitivity to increased ramping constraints, based on values for 2018. The initial values can be seen in the legend. . . . .	32
Figure 22	Resulting capacities and annual costs for various models. In model 1-3 the system has an air-sourced heat pump, while the heat pump in model 4 and 5 is ground-sourced. . . . .	35
Figure 23	Maximum cost increases for the models run for the years 2013-2019 without electricity cost optimisation. . . . .	37
Figure 24	The energy system is modelled for fixed capacities to examine the dynamics of the current system and determine the impact of electrifying the district heating sector. . . . .	38
Figure 25	As Samsø aims to increase the VRES capacities in the future, the energy system is allowed to increase the installed capacity in this stage. Again the system is modelled in steps to see what happens as sector coupling increases. Lastly, the impact of the expected cost-reduction towards 2050 and the possibility of expanding the link to DK1 is examined. . . . .	39
Figure 27	Average monthly capacity factors for Samsø and Denmark. The capacity factors on Samsø are consistently higher than the average capacity factor across Denmark. . . . .	40
Figure 28	Average weekly electricity generation and demand on Samsø. The annual renewable generation on Samsø is six times larger than the annual electricity demand. . . . .	40
Figure 26	Fourier power spectrum for solar PV and wind generation. Solar PV is dominated by the daily frequency, while the annual variation dominates wind generation. . . . .	41
Figure 29	As Samsø has a large amount of renewable capacity installed, the export of electricity is far greater than the import, but the import is necessary to meet the electricity demand on Samsø. . . . .	41
Figure 30	Average weekly electricity production and consumption on Samsø. The electricity demand increases when the electricity and heating sectors are coupled, and the electricity demand takes the shape of the heat demand. . . . .	42

Figure 31	Average daily heat production and heat demand for the district heating sector on Samsø. The large plant (top) is modelled separately, while the three small district heating plants are modelled as one aggregated plant.	43
Figure 32	Duration curves for the link flow in the current energy system and a coupled electricity and heating sector. The export reduces when the electricity and heat sector are coupled, and in the peak import hours the flow doubles.	44
Figure 33	Capacities on Samsø for the 7 years modelled. Most years the capacities are not increased, but for two years with a slightly higher capacity factor for solar PV, the installed capacity is increased significantly.	45
Figure 34	The link flow for the optimal capacities for the last half of March in 2018. Electricity is occasionally curtailed due to either link capacity or spotprices.	45
Figure 35	Overview of the total electricity generation on Samsø in 2018. Most of the electricity generation on Samsø is exported to DK1, part of it is used to cover the islands electricity demand, and a small part is curtailed.	46
Figure 36		46
Figure 37	Expected cost decrease for hydrogen storage towards 2050. Further increase in associated costs have also been tested.	47
Figure 38	Hotmaps for the transport demand, charge and discharge, and electricity spot prices in 2018.	48
Figure 39	Link flow before and after the transport sector is coupled to the electricity sector.	49
Figure 40	Fourier power spectrum for the transport demand, electricity spot price, and transport storage charge and discharge.	50
Figure 41	Annual curtailment before and after transport sector coupling. Curtailment is only reduced for the years with increased solar capacity.	50
Figure 42	Hourly export and curtailment for a selected week in may 2013. Here it can be seen how the reduction in curtailment occurs when electricity is curtailed due to export limitations.	51
Figure 43	Expected cost decrease for the included renewable generation technologies, taken from the Danish Energy Agency (DEA) Technology Database [1] and artificial decrease in wind costs.	51
Figure 44	Installed capacity for 2020-2050. The optimal capacities are first found for the current link, then the model is allowed to increase the transmission capacity, and finally the constraint for the allowed solar PV capacity is removed.	52

Figure 45	Detailed overview of the model for the coupled electricity and heating sector on Samsø with the possibility of hydrogen storage. . . . .	67
Figure 46	Detailed overview of the model for the coupled electricity and heating sector on Samsø. . . . .	68
Figure 47	Detailed overview of the model for the coupled electricity, heating, and transport sector on Samsø with the possibility of hydrogen storage. . . .	69

## LIST OF TABLES

---

Table 1	Data for Samsø provided by Statistics Denmark [2]. . . . .	1
Table 2	Time series data used in the optimisations. Due to the limits for the time series data the models is only run for the years 2013-2019. The average monthly ground temperature at a depth of 1 meter is given for several locations in Denmark by [3]. In the model, the average temperature for all locations is used.. . . . .	6
Table 3	Overview of symbols used in the objective function for PyPSA. . . . .	7
Table 4	Overview of currently installed VRES, given by Østergaard et al. in [4], and the maximum allowed capacity. . . . .	8
Table 5	Cost assumptions for various types of renewable electricity generation taken from the Danish Energy Agency (DEA) Technology Database [1] .	9
Table 6	Electricity fees and levies added to the hourly spotprice when electricity is purchased from the grid. . . . .	10
Table 7	Cost and lifetime of link expansion, increasing the possible export to from Samsø to DK1 . . . . .	10
Table 8	Data for heat generation technologies from the Danish Energy Agency (DEA) Technology Database [1] & [5].The heat pumps are all air sourced and the variable O&M for heat pumps and resistive heater does not include electricity costs. . . . .	12
Table 9	Data for heat storage from the Danish Energy Agency (DEA) Technology Database [6]. . . . .	12
Table 10	Capital cost increase for the heat pumps in the district heating sector when the temperature increases or the heat source changes. . . . .	13

Table 11	Information on the included heating demands. The rated heat demands for the DH plants are given in [4]. These are converted to the rated heat production for each plant from the grid efficiency. The individual heat demand is calculated in Appendix A and the required energy for hourly hot water for each demand is calculated as in Section 2.4.3. The scaling factor is used to calculate the annual heat production for each of the years from the values for BBDH provided by [7]. . . . .	14
Table 12	Resulting $\chi^2$ -values for different threshold temperatures. With a maximum allowed $\chi^2$ -value of 19.8, any threshold temperature above 14.5°C leads to an accepted fit, but a threshold temperature of 16°C gives the lowest $\chi^2$ -value. . . . .	17
Table 13	Values used for calculating the COP. . . . .	18
Table 14	Data for renewable energy conversion technologies. Assumptions are taken from the Danish Energy Agency (DEA) Technology Database, [1] and [8]. . . . .	22
Table 15	Data for hydrogen storage. Assumptions are taken from catalogues published by the Danish Energy Agency (DEA) Technology Database [6].	23
Table 16	Data for the BEV's included in the model . . . . .	24
Table 17	Data for the BEV's included in the model . . . . .	25
Table 18	Resulting capacities and costs for the model run for the years 2013-2019	33
Table 19	Comparison between resulting capacities and costs for constant and varying COP calculated from data for 2018. . . . .	33
Table 20	Comparison between resulting capacities and costs for ASHP with and without storage. . . . .	34
Table 21	Comparison between resulting capacities and costs for air-sourced and ground-sourced heat pumps with varying COP. . . . .	34
Table 22	Recommended capacities for the systems with air-sourced and ground-sourced heat pumps. Capacities are calculated with a safety factor of 1.5 for the heat pump and 2 for the cheaper resistive heater and heat storage.	36
Table 23	Values for 2018 . . . . .	48
Table 24	The onshore production is on average 40% higher than the historic production, when using the capacity factors taken from [9] directly. . .	65
Table 25	The modelled offshore production matches the historic production better than the onshore production, suggesting that the island of Samsø is not captured in the model generating the capacity factors. . . . .	65

# 1 INTRODUCTION

---

As the Renewable Energy Island of Denmark, Samsø is an interesting focal point for any researcher interested in energy and the transition towards a greener future. This small island has received international attention and prizes and was recently awarded second place in the RESponsible Island 2019-awards [10] for the continuous work done by the island's Energy Academy.

The project that landed Samsø the title of Renewable Energy Island, now referred to as Version 1.0, was to become 100% self-sufficient with renewable energy. This project was completed in just ten years, and the key factors to its success were examined in [11].

The next project, Version 2.0, was set in place in 2009 and defined the path of the island's energy system towards 2030. The goals of this project include becoming independent of fossil fuels, maintaining and expanding renewable electricity production, and reducing losses in the heating sector.

## 1.1 THE ISLAND OF SAMSO

Samsø is a small island in Kattegat, connected to both Jutland and Zealand by ferries. The island has just above 3,500 permanent residents. It is also a popular holiday destination with almost as many vacation homes as households on the island, as seen in Table 1.

While the tourist industry on Samsø is booming, not much traditional industry is present on Samsø. Instead, the island is dominated by agriculture, and this sector, along with the transport sector, produces nearly all Samsø's CO<sub>2e</sub>-emissions. The transport sector alone emits 22,500 ton CO<sub>2e</sub>, the majority as a result of the island's ferries, and the agricultural sector contributes with an extra 20,000 ton CO<sub>2e</sub> [12].

**Table 1:** Data for Samsø provided by Statistics Denmark [2].

Residents	Households	Vacation homes
3,684	1,977	1,682

1.2 RENEWABLE ENERGY ISLAND

Since Samsø was named the Renewable Energy Island of Denmark in 1997, many actions have been taken to transition the island towards a greener future. In Version 1.0, the district heating sector on Samsø was expanded, and on- and offshore wind turbines were installed to generate enough electricity to cover the island’s demand and export electricity to the mainland. Furthermore, one of the ferries connecting Samsø and Jutland has already been converted to be powered by natural gas [13]. By 2030, the ferry connecting Samsø to Zealand will be converted to natural gas, and the smaller ferry connecting Samsø to Aarhus will be fuelled by renewable fuel by 2050 [12].

Plans for the island also include installing a large solar power plant and constructing a biogas plant to power the island’s ferries and other heavy traffic. An overview of existing and proposed infrastructure can be seen in Fig. 1.

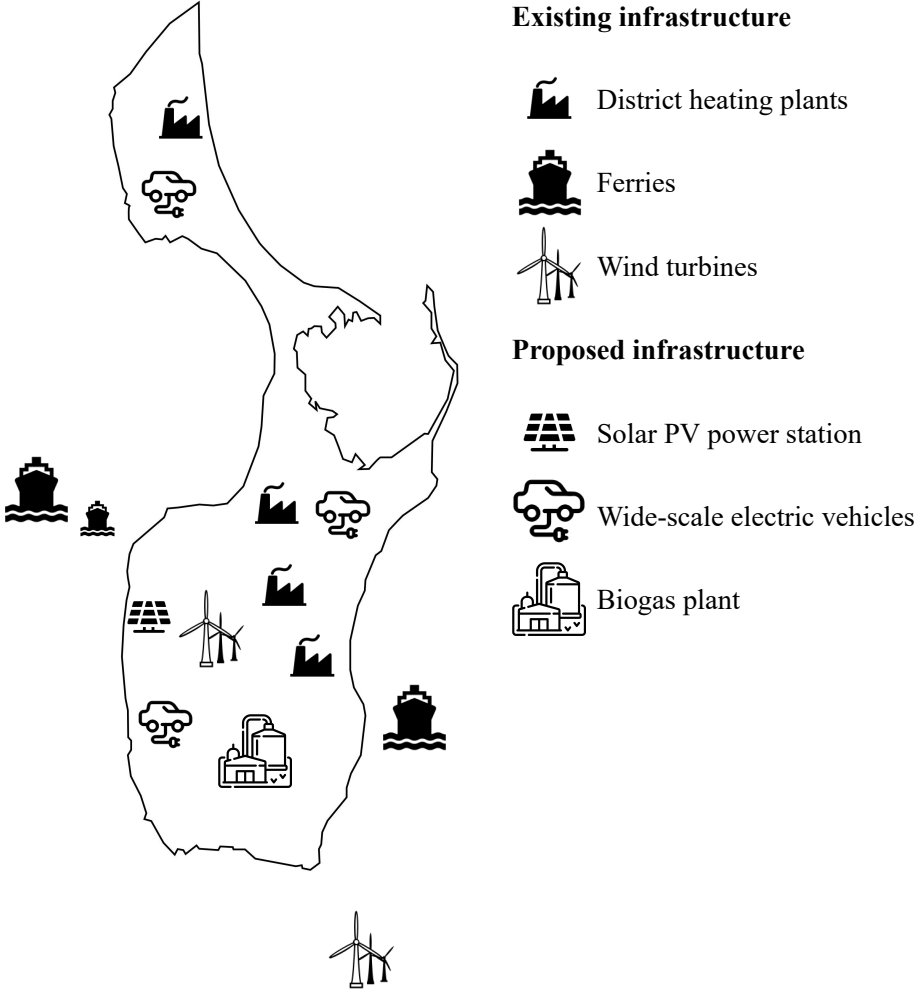


Figure 1: Overview of installed and proposed infrastructure in the energy sector on Samsø.

The idea of a local biogas plant has not always been popular among the residents of the island [14]. However, since the island's recently published climate plan showed that the island is no longer CO<sub>2</sub>-neutral, the remaining adversaries could be swayed in favour of the plant. Notably, the cause for the retraction of Samsø's status as CO<sub>2</sub>-neutral is the inclusion of the fossil fuels used by the ferries and the agricultural sector, which a biogas plant could replace.

While the municipality of Samsø still has the highest share of renewable energy in the region, with a renewable penetration of 70,8% [15], being the best in the region is not enough for Denmark's Renewable Energy Island.

With the plans for a local biogas plant closer to becoming a reality, the plant's demand for biomass must be addressed. A significant part of the island's biomass is utilised in the district heating sector, as three out of the island's four district heating plants are fuelled by straw. Given that the island wishes to avoid the increased cost and associated CO<sub>2</sub>-emission generated by importing biomass, the biogas plant will lay claim to the local biomass used to fuel the straw boilers in the district heating sector. A reformation of the island's district heating plants is therefore required.

In [4] the electrification of the district heating sector on Samsø was examined. Here the biomass boilers were replaced by heat pumps and resistive heaters to increase consumption of the locally generated electricity from the wind turbines.

Heat pumps are gaining a foothold in the Danish district heating sector for an excellent reason, as heat pumps are a CO<sub>2</sub>-neutral way to generate heat, as long as the electricity is produced from renewable sources. In addition to this, heat pumps are also highly efficient compared to biomass boilers, producing around 3 MW heat for every 1 MW of electricity.

The study by Østergaard et al. [4] determined that electrification of the district heating sector could increase local wind power usage, decrease the load on the transmission link, and free up the local biomass for use in a biogas plant. However, the operation of a heat pump based district heating plant was not cost-competitive with biomass boilers.

Since this study was completed, a decrease in the levies placed on electricity used for heating purposes has been introduced [16]. This decrease, along with increasing maintenance costs of the district heating plant previously examined in [4], makes it relevant to reexamine the future of district heating on Samsø. As the straw boiler in the district heating plant, established in 2005 [17], is nearing the end of its lifetime, and residents are complaining about smoke pollution [7], now is time to review the electrified heating plant.

### 1.3 PROJECT OUTLINE

The purpose of this project is to answer the following research questions:

*Is the production cost for an electrified district heating plant cost-competitive with biomass burners?*

*What are the effects of increasing synergy between the energy sectors on Samsø?*

*Can Samsø benefit from increasing its renewable capacities?*

To do this, the project is examined in two parts. First, a techno-economical analysis is done to establish the optimal configuration for an electrified district heating plant. The plant's operation is examined and further investigated how sensitive the optimal capacities are to several variations in input. This sensitivity analysis is done to ensure that the recommended capacities for the system can cover the demand in any situation.

In the second part, the islands current and future energy systems are modelled. The current system is studied to determine the impact of electrifying both the district heating sector and the remaining fossil-fuelled part of the private heating sector. The near-future system is examined to determine if it is cost-optimal for the island to expand its renewable generation and how the storage capacity of an electrified transport sector can help balance the VRES and fluctuation electricity spot price.

Moreover, it is explored how the expected development in cost associated with the installation and maintenance of renewable generation influence the optimal expansion of the installed VRES capacity on the island.

## 2 METHODS

---

The purpose of this chapter is to disclose the assumptions for the project, give a brief review of the optimisation algorithm used, and outline the various input used in the models.

### 2.1 ASSUMPTIONS

Any time a system is examined, aspects are excluded, and assumptions are made to simplify the system and make it possible to model.

In this project, the model assumes infinite transmission capacity within the island, with the connection to the mainland being the only limited transmission link. Historical production and consumption are assumed to continue in the future. Therefore, growth in electricity demands, changes in weather patterns, and variation in the island's population are excluded.

Additionally, all cost estimations, apart from the section for cost reductions in Section 4.2.4, are based on 2020. This is chosen on the assumption that Samsø wants to maintain its image as a Renewable Energy Island. As such, changes must be made before the CO<sub>2</sub>-quotas ends in 2030.

Lastly, the time-dependent input is found with an hourly resolution when possible, and an overview and the source of this data can be seen in Section 2.1. Some data is only available for a limited number of years, and as a result, the models are only examined for the years 2013-2019. As Samsø is a small island, time-series data with an hourly resolution for Samsø is not readily available. Therefore, this data is modelled by scaling corresponding hourly data. These calculations can be found for wind generation and electricity demand in Appendix B.

Since the ground temperature varies very little compared to the air temperature, the average monthly data for 2001-2010 is assumed to correspond to all modelled years.

**Table 2:** Time series data used in the optimisations. Due to the limits for the time series data the models is only run for the years 2013-2019. The average monthly ground temperature at a depth of 1 meter is given for several locations in Denmark by [3]. In the model, the average temperature for all locations is used..

	Resolution	Years	Source
Air temperature	Hourly	1980-2019	[9]
Ground temperature	Monthly	2001-2010	[3]
Solar PV capacity factor	Hourly	1980-2019	[9]
Wind capacity factors	Hourly	1980-2019	[9]
Elsport prices DK1	Hourly	2013-2020	[18]
Electricity demand DK1	Hourly	2013-2020	[18]
Historical heat production for BBDH	Monthly	2011-2020	[7]

## 2.2 PYTHON FOR POWER SYSTEM ANALYSIS

Python for Power System Analysis (PyPSA) is used to model and optimise the systems. Here the system objective is to minimise the total annual system cost by optimising capacities and dispatch for each model.

The objective function for the system can be seen in Eq. (1). The system costs are split into capital and operational costs for generation, storage, transmission and conversion. Descriptions of the symbols included in the objective function are explained in Table 3.

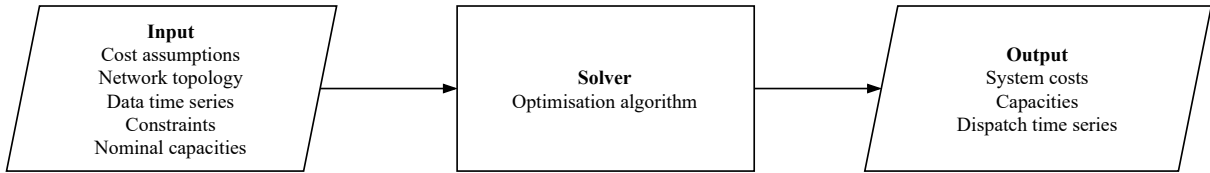


**Figure 2:** Cost optimisation in PyPSA.

$$\min_{\substack{G_{n,s}, g_{n,s,t}, \\ E_{n,r}, F_l}} \left[ \underbrace{\sum_{n,s} c_{n,s} \cdot G_{n,s}}_{\text{Generation capital costs}} + \underbrace{\sum_{n,s,t} o_{n,s,t} \cdot g_{n,s,t}}_{\text{Generation operational costs}} + \underbrace{\sum_{n,s} c_{n,s} \cdot E_{n,s}}_{\text{Storage capital costs}} + \underbrace{\sum_l c_l \cdot F_l}_{\text{Transmission capital costs}} \right] \quad (1)$$

**Table 3:** Overview of symbols used in the objective function for PyPSA.

Symbol	Description
$c_{n,s}$	Fixed annualised cost for each node, $n$ , and generation technology, $s$
$G_{n,s}$	Installed generation capacity for each node and technology
$o_{n,s,t}$	Marginal cost for generation and storage dispatch for every timestep, $t$
$E_{n,s}$	Installed storage capacity for each node and technology
$c_l$	Fixed annualised cost for each transmission link, $l$
$F_l$	Transmission capacity for each link

Each model is solved for a full year in hourly snapshots. As the capital costs for the components are distributed over their lifetimes, all capital costs are annualised using Eq. (2). This equation also includes a discount rate, accounting for inflation and associated risks, when calculating the annual cost of investing in a component. For all investments, the discount rate is assumed to be 7%.

As the snapshots modelled for the system are hourly, energy production and consumption are described by MWh, while the capacity of generation and links are specified by MW.

$$A = C \frac{r(1+r)^n}{(1+r)^n - 1} \quad \left\{ \begin{array}{l} r = \text{discount rate} \\ n = \text{lifetime} \\ A = \text{annualised cost} \\ C = \text{Capital cost} \end{array} \right. \quad (2)$$

## 2.3 ELECTRICITY

In this section, a summary of the current electricity system on Samsø is given, and the allowed increase in renewable capacity is established. The cost assumptions are specified for renewable generation technologies and link expansion, and the included fees and levies paid when purchasing electricity from the grid are defined.

### 2.3.1 Electricity system on Samsø

The current electricity system on Samsø consists exclusively of renewable generation. The installed capacity consists of mainly on- and offshore wind, aided by a small amount of solar PV, as seen in Fig. 3. The island is connected to the mainland by a 40 MW transmission link. This link is used to sell electricity to DK1 or import electricity purchased from the grid when

Samsø cannot generate electricity enough to support the demand on the island, which totals 21.5 GWh/year [4].

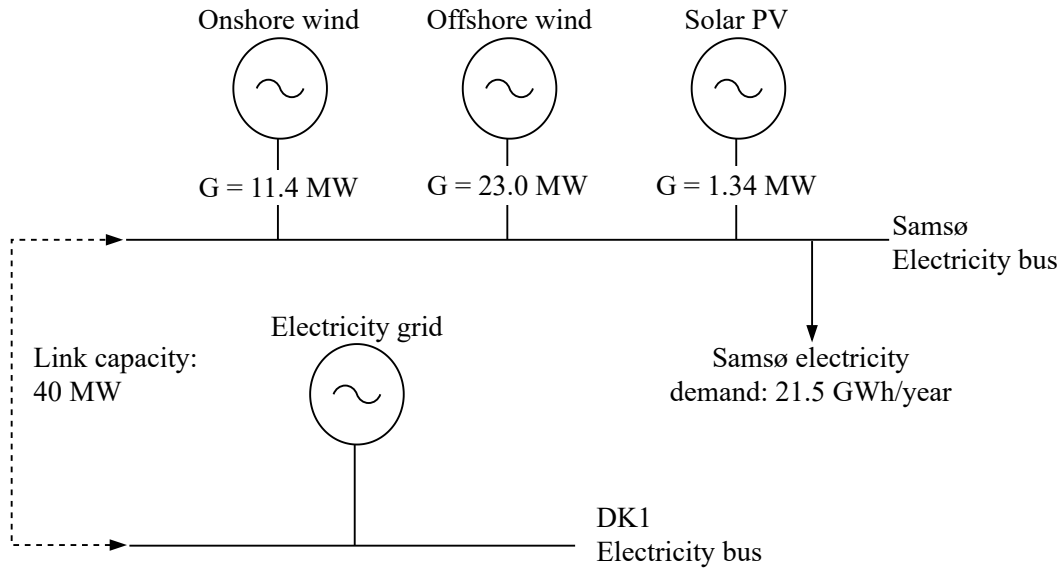


**Figure 3:** Overview of the current electricity system on Samsø.

### 2.3.2 Capacities

While the renewable capacities on Samsø are more than enough to generate enough electricity to cover the annual electricity demand on the island, an optimisation, where the installed capacity is allowed to increase, could result in unreasonably high capacities. Therefore, maximum capacities are defined for each technology to limit the installation of renewable capacities on Samsø to realistic levels.

**Table 4:** Overview of currently installed VRES, given by Østergaard et al. in [4], and the maximum allowed capacity.

Description	Current capacity	Maximum capacity
Solar PV	1.34 MW	81.3 MW
Onshore wind	11.4 MW	69.0 MW
Offshore wind	23.0 MW	65.0 MW

The study by Sperling [11] states that 40 local property owners applied to have wind turbines on their land when the 11 onshore wind turbines were installed in 2000. It is assumed that the remaining 29 property owners, who were not selected 20 years ago, are still interested in

installing wind turbines on their land. As the small onshore wind turbines are now rated at 2 MW [19], rather than 1 MW, this allows for an increase in onshore capacity of 58 MW. Thus, including the current capacity, the maximum onshore wind capacity is 69 MW.

Regarding offshore capacity, it could be possible to install another offshore plant of 10 turbines. With a current rating for the small near-coast turbines of 4.2 MW [19], this allows for an increase of 42 MW. The maximum allowed offshore capacity, therefore, amounts to 65 MW.

For solar capacity, an increase in 80 MW is allowed. This limit is chosen as it corresponds to the solar power plant proposed in [20] and along with the current capacity, the maximum allowed capacity totals 81.3 MW.

### 2.3.3 Cost assumptions for renewable electricity generation

As the purpose of PyPSA is cost-optimisation, the defined costs for generators and components must reflect reality. To ensure this, the cost assumptions are taken from the Danish Energy Agency's technology database. These can be seen in Table 5.

When looking at wind generation, the cost of offshore wind is twice the cost of onshore, and even though the capacity factor for offshore wind is higher than for onshore, it is not twice as high. This means that offshore wind will likely only be included when/if the maximum allowed capacity for onshore wind is reached.

**Table 5:** Cost assumptions for various types of renewable electricity generation taken from the Danish Energy Agency (DEA) Technology Database [1]

	Onshore wind	Offshore wind	Solar PV	Unit
Typical rating	4.2	10	8	MW
Lifetime	27	27	35	years
Capital cost	1.12	2.13	0.53	2015-M€ /MW
Fixed O&M	14,000	40,059	8,750	2015-€ /MW
Variable O&M	1.50	3.0	-	2015-€ /MWh

### 2.3.4 Electricity fees

When purchasing electricity from the grid, various fees and levies are added on top of the hourly spot price given by [18]. However, the electricity levy is not included in the model, as the electricity is used for heat production, for which electricity levies have been reduced [7].

Therefore, the included fees and levies are limited to the PSO levy, the distribution grid fee and the transmission grid fee, the values of which can be seen in Table 6.

When the energy system on Samsø connected to DK1 is modelled, all levies and fees are excluded from the generators. These are paid by the consumers and assumed identical in DK1 and on Samsø. However, the levies and fees are added to the marginal costs for the heat pumps and resistive heaters in the district heating sectors, as the electricity price affects the optimal ratio of these.

**Table 6:** Electricity fees and levies added to the hourly spotprice when electricity is purchased from the grid.

PSO levy	Distribution grid fee	Transmission grid fee	Total	Unit
4.71	27.98	8.88	41.58	EUR/MWh

### 2.3.5 Link expansion

The limiting factor for increasing renewable capacity on Samsø, besides the allowed capacities defined in Section 2.3.2, is the link connecting the island to the mainland. This link is currently limited to 40 MW, but it is relevant to examine if it pays off to expand this link to produce more electricity on Samsø, which can then be sold to DK1. From values found in [21] cost of a link for main electricity distribution with a capacity between 0-50 MW is calculated from an approximate distance between Samsø and Jutland of 18.5 km. However, the exact length depends on the cable placement. The resulting costs can be seen in Table 7, and these are likely on the low side, as the Danish Energy Agency has not included cost for ocean cables, but as the possibility of a bridge over Samsø is currently being examined, the costs will likely hold if this becomes a reality.

**Table 7:** Cost and lifetime of link expansion, increasing the possible export to from Samsø to DK1

Capital cost	Station cost	Fixed O&M	Lifetime
0.111 M€ /MW	76,000 € /MW	409 € /MW	40 years

## 2.4 HEATING

In this section, the model for an electrified district heating plant is described, and cost assumptions for the included technologies are specified. The heat demand for the Ballen-Brundby district heating plant is modelled, and the hourly COP for the heat pump is calculated. Calculations on the individual heat demands can be found in Appendix A.

### 2.4.1 Model overview

In the electrified district heating plant, heat is produced by a heat pump and a resistive heater. The heat production is balanced by thermal energy storage (heat storage) in the form of a large water tank. Electricity is purchased directly from the grid at the hourly spot price with the included fees and levies mentioned in Table 6.

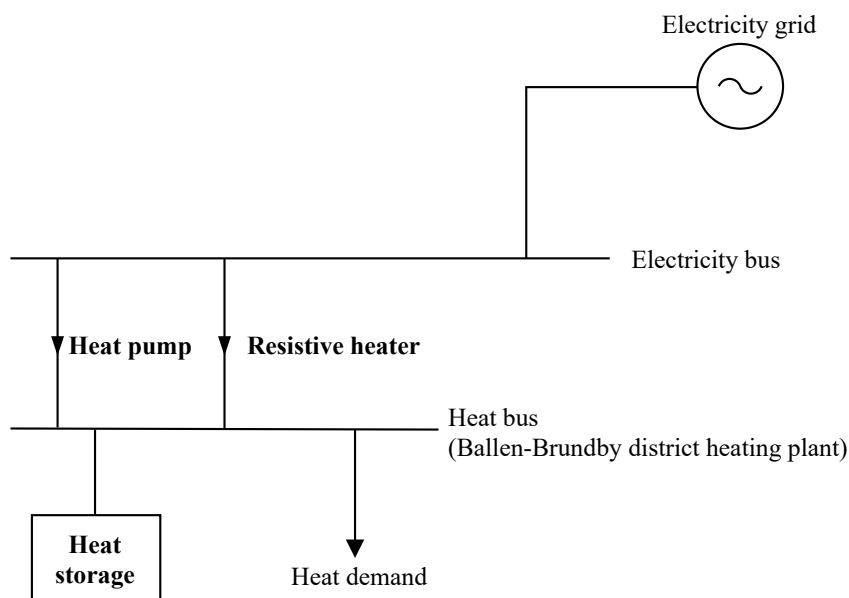


**Figure 4:** System model for BBDH. Capacity and dispatch are optimised for the components marked in bold.

### 2.4.2 Cost assumptions for heat generation and storage technologies

Cost assumptions for the heat generation and storage is taken from catalogues published by the Danish Energy Agency for individual heating [5], district heating [1], and energy storage

[6]. Data is given for three different heat pump sizes, as cost varies with the rating. Heat pumps are therefore split into three different categories; individual heat pumps, small scale DH heat pumps and medium scale DH heat pumps. Cost assumptions for heat generation is given in Table 8 and for storage in Table 9

**Table 8:** Data for heat generation technologies from the Danish Energy Agency (DEA) Technology Database [1] & [5]. The heat pumps are all air sourced and the variable O&M for heat pumps and resistive heater does not include electricity costs.

	Individual heat pumps	Small scale DH heat pumps	Medium scale DH heat pumps	Resistive heater	Unit
Typical rating	0.009	1	3	0.06-5	MW
Name plate COP	315	255	310	99	%
Lifetime	16	25	25	20	years
Minimum load	25	25	25	5	% of full load
Capital cost	1.2	1.4	0.95	0.15	2015-M€ /MW
Fixed O&M	34,556	2,000	2,000	1,070	2015-€ /MW/year
Variable O&M	-	2.7	2.2	0.5	2015-€ /MWh

**Table 9:** Data for heat storage from the Danish Energy Agency (DEA) Technology Database [6].

	Heat storage	Unit
Energy storage capacity for one unit	175	MWh
Energy losses during storage	0.2	% / day
Energy losses during storage	0.00834	% / hour
Lifetime	40	years
Capital cost	3,000	2015-€ /MWh
Fixed O&M	8.6	2015-€ /MWh/year

When the system temperatures increase or the heat source changes, the capital cost will increase. The cost-increase for temperature changes is given by [1] and is due to higher pressures in the system. The higher pressure requires particular components of a higher quality. The cost increase for ground-sourced heat pumps is estimated based on the cost ratio for air- and ground-sourced heat pumps used in [22]. Both cost increases can be seen in Table 10.

**Table 10:** Capital cost increase for the heat pumps in the district heating sector when the temperature increases or the heat source changes.

	Small scale HP	Medium scale HP	Unit
Capital cost increase for 40/80°C systems	15	10	%
Capital cost increase for ground-sourced heat pumps	60	60	%

### 2.4.3 Heat demand modelling

Unlike electricity demand, hourly historical data for heating demand is not readily available. Therefore, the hourly heat production for BBDH is instead modelled by splitting the heat production into three categories; a constant demand for hot water, a constant grid loss, and a varying demand for space heating calculated from the hourly temperature. These are determined in the following subsections.

Similar estimations are made for the DH plant in Tranebjerg and the total heat production for the other small DH plants on Samsø. These smaller DH plants and BBDH will be modelled as one aggregated plant in the later analysis of the collective energy system on Samsø. An overview of the heat demands included in the collective energy system on Samsø can be seen in Table 11 along with the factors used to scale the historical production for BBDH.

The modelled heat production for BBDH, calculated in the following sections, is compared to the historical monthly production to establish the best threshold temperature for the space heating demand. It is assumed that the modelled heat production for the remaining DH plants fit as well as it does for BBDH, as the limited historical data for the remaining DH plants on Samsø make it impossible to evaluate the fit of these.

#### *Hot water demand*

The demand for hot water (HWD) is estimated from the total annual energy used for hot water in Denmark in 2015, given by [23]. This annual demand is scaled to match the number of households in the BBDH grid. The demand for hot water is set to be constant for every hour of the year as it is assumed that the hot water tank can easily cover the peak loads in the morning and evening.

**Table 11:** Information on the included heating demands. The rated heat demands for the DH plants are given in [4]. These are converted to the rated heat production for each plant from the grid efficiency. The individual heat demand is calculated in Appendix A and the required energy for hourly hot water for each demand is calculated as in Section 2.4.3. The scaling factor is used to calculate the annual heat production for each of the years from the values for BBDH provided by [7].

	BBDH	Tranebjerg	Small total	Individual demand	Unit
Rated heat production	5.63	13.40	18.8	15.9	GWh
Scaling factor	-	2.38	3.34	2.82	-
Grid efficiency	0.67	0.71	0.71	-	-
Consumers	300	400	620	644	-
Hourly hot water demand	69.2	92.3	143	149	kWh

First the hourly hot water demand for an average household is calculated in Eq. (3).

$$\begin{aligned}
 \text{HWD per household} &= \frac{\text{yearly demand in DK}}{\text{households in DK} \cdot 8760 \text{ hours}} \\
 &= \frac{5,512,620 \text{ MWh}}{2,728,132 \cdot 8760 \text{ hours}} = 0.231 \text{ kWh}
 \end{aligned}
 \tag{3}$$

The hourly hot water demand for BBDH is calculated by scaling the average household demand to the 300 households connected to the district heating plant.

$$\begin{aligned}
 \text{HWD for Ballen-Brundby DH} &= 0.2307 \text{ kWh} \cdot 300 \text{ households} \\
 &= 69 \text{ kWh}
 \end{aligned}
 \tag{4}$$

With 300 households connected to the Ballen-Brundby district heating plant, this gives a constant hourly demand for hot water of 69 kWh.

#### *Grid loss*

The grid consists of 7 kilometres of pipes, leading to a significant heat loss in the grid due to the temperature difference between the hot water and the ground temperature. For BBDH, this corresponds to 33% of the annual production [17]. As the hot water temperature is constant throughout the year, and the ground has limited temperature variation at the depth where the DH pipes are placed, this loss is assumed to be constant for every hour of the year.

As the annual heat production varies from one year to the next, the constant hourly grid loss (HGL) is calculated for each year, the same way it is calculated for 2019 in Eq. (5).

$$\text{GL for Ballen – Brundby DH} = \frac{5576 \text{ MWh} \cdot 0.33}{8760 \text{ hours}} = 210 \text{ kWh} \quad (5)$$

### Space heating demand

Heating degree hours (HDH) are used to estimate the demand for space heating from the temperature. Modelled temperatures from [9] is used, as hourly measured temperature for Samsø is not readily available. As these temperatures are not the actual measured temperatures on Samsø, they are compared to the measured temperatures from DMI in Fig. 5.

The mean temperatures are a near-exact match, but the maximum and minimum temperatures are not captured precisely by the model temperature. This is not considered a significant issue for the space heating estimation, as the minimum and maximum temperatures follow the same trend as the measured temperature, and the HDH are scaled to the annual historical production. Nevertheless, the fact that the minimum temperature is not captured precisely does reduce the heat pumps temperature dependant COP. However, the safety factor used to calculate the recommended heat pump and resistive heater capacity will account for this.

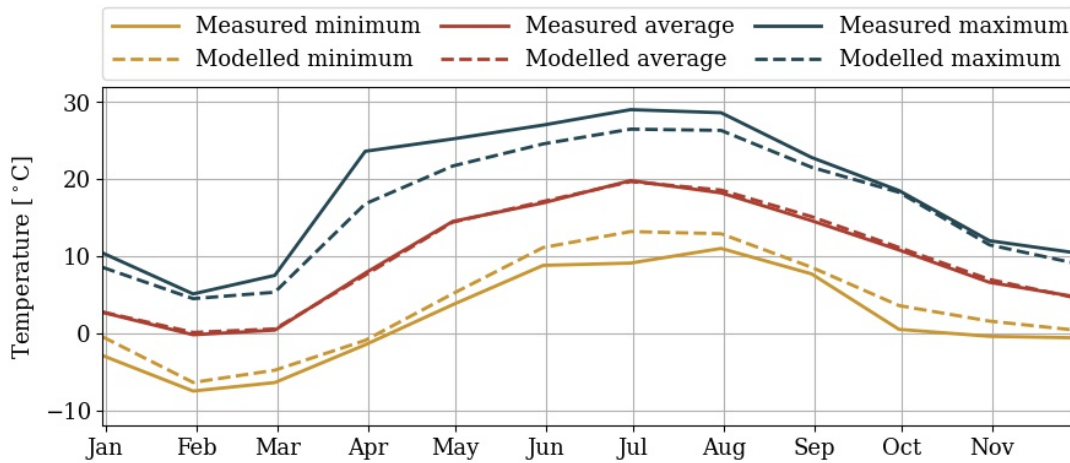


**Figure 5:** Comparison between measured and modelled temperatures.

When calculating heating degree hours, it is assumed that there is no need for space heating when the temperature is above a selected threshold temperature. As the temperature decreases below this threshold, the HDH increases linearly, as seen in Eq. (6).

$$HDH_t = \begin{cases} 0 & \text{if } T_{ambient} > T_{threshold} \\ (T_{threshold} - T_{ambient}) & \text{if } T_{ambient} < T_{threshold} \end{cases} \quad (6)$$

To find the hourly space heating demand, SHD, from the heating degree hours, these are scaled with a scaling factor,  $C$ , to match the total annual demand for space heating.

$$SHD_t = HDH_t \cdot C \quad (7)$$

$$C = \frac{\text{annual heat production} - (\text{HWD} + \text{GL}) \cdot 8760 \text{ hours}}{\sum_t HDH_t} \quad (8)$$

### The $\chi^2$ Goodness of Fit Test

As data for the historical monthly heat production is available, a  $\chi^2$  goodness of fit test is used to determine which threshold temperature leads to the best fit. This fit is then evaluated to check how well the modelled monthly heat production fits the historical production.

$\chi^2$  is calculated from the observed historical value  $O_i$  and the expected modelled value  $E_i$  as seen in Eq. (9). The lower the  $\chi^2$ -value is, the higher the corresponding correlation between the model and the historical data.

$$\chi^2 = \sum_i \frac{(O_i - E_i)^2}{E_i} \quad (9)$$

The statistical significance is set to 5%, and the null hypothesis for the test is that the modelled heat production describes the actual historical production. This hypothesis is rejected if the resulting  $\chi^2$  is higher than the limit of 19.7.

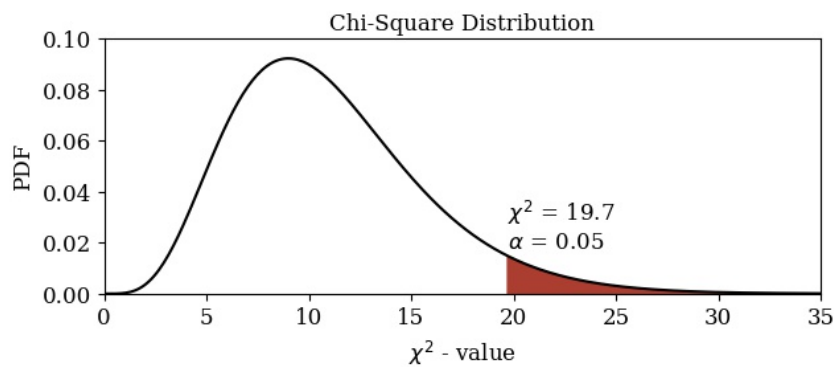


**Figure 6:**  $\chi^2$ -distribution for 11 degrees of freedom and critical values.

The test is run for the years 2013-2019 with threshold temperatures varying from 14.0°C to 17.5°C to find out which threshold temperature leads to the lowest average  $\chi^2$  value. The result of this can be seen in Table 12, where a threshold temperature of 15.0°C or higher leads to an average  $\chi^2$  below the accepted limit, with 16.0°C leading to the best fit.

The resulting modelled monthly heat production is compared to the actual historical production for the two years with the lowest and highest  $\chi^2$  in Fig. 7. Here it can be seen that even the year with the highest  $\chi^2$  still show a high overlap between modelled and historic heat production.

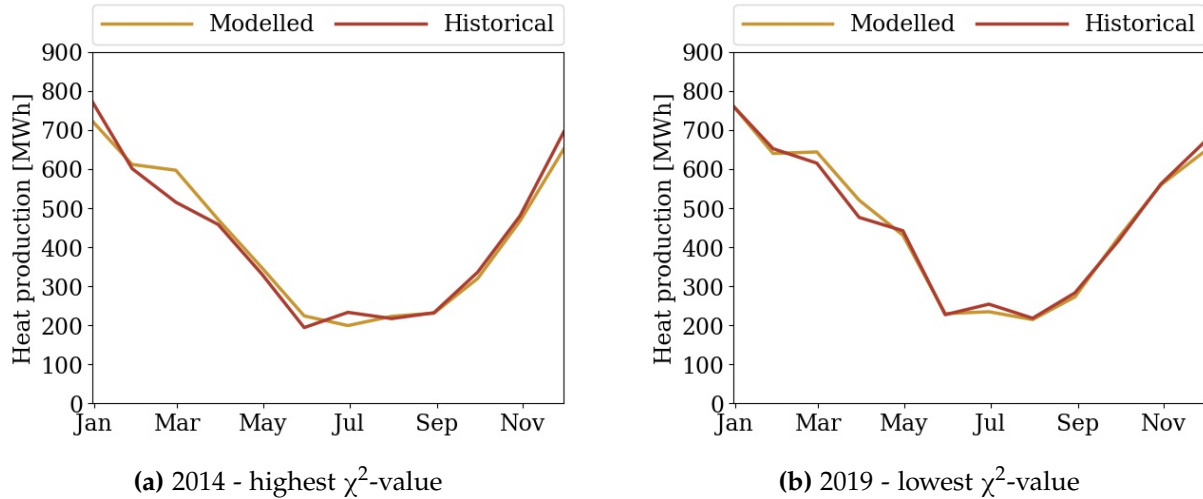


**Figure 7:** Comparison between historic and modelled heat production for the highest and lowest  $\chi^2$  values for a threshold temperature of 16°C.

#### Total heat production

The total resulting heat production in 2018 for the three categories can be seen in Fig. 8 where the grid loss and hot water demand remains constant for every hour of the year, while the hourly demand for space heating has a clear seasonality, with high demand in the colder months, and barely any demand during the summer.

#### 2.4.4 Heat pumps

In this section, the Coefficient Of Performance (COP) of the air-sourced and ground-sourced heat pump will be calculated. Furthermore, the air-sourced heat pump's issue with low

**Table 12:** Resulting  $\chi^2$ -values for different threshold temperatures. With a maximum allowed  $\chi^2$ -value of 19.8, any threshold temperature above 14.5°C leads to an accepted fit, but a threshold temperature of 16°C gives the lowest  $\chi^2$ -value.

Threshold temperature	14.0°C	14.5°C	15.0°C	15.5°C	16.0°C	16.5°C	17.0°C	17.5°C
Average $\chi^2$	37.8	26.4	17.7	11.9	8.99	9.08	12.1	18.0

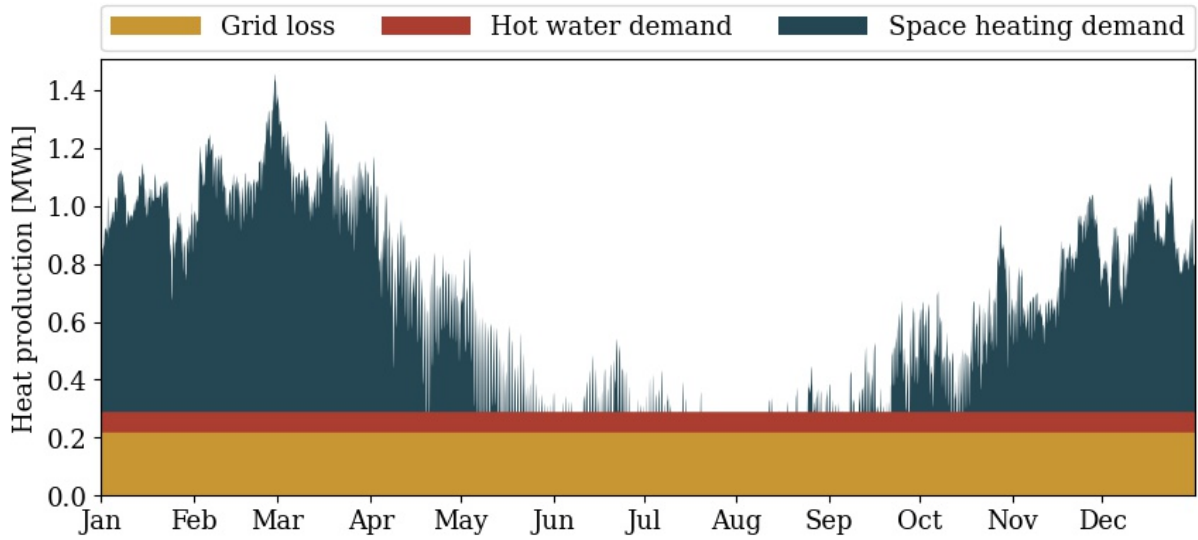


**Figure 8:** Hourly heat production for each category for 2018.

temperatures is examined to ensure that the temperatures on Samsø are not an issue for the heat pumps performance.

#### *COP for air-sourced heat pump*

While [1] states the heat pumps nameplate COP as 2.55, this value is given for a heat pump operating with a return/forward temperature of 35°C/70°C and an air temperature of -1°C. It also includes energy consumption for defrosting and auxiliary electricity consumption.

In this section, both the corresponding nameplate COP and the temperature dependant COP will be calculated for a system with a return/forward temperature of 40°C/80°C as is the case for BBDH as noted in [17].

The nameplate and varying COP are calculated from Eq. (10) and Eq. (11), the values given in Table 13, and the temperature data from [9].

**Table 13:** Values used for calculating the COP.

	Description	Symbol	Value	Unit	Source
	Cooling of air through cooling surfaces	$\Delta T_{source}$	5	K	[1]
	Temperature of water returning from consumers	$T_{return}$	40	°C	[17]
	Temperature of water leaving the district heating plant	$T_{forward}$	80	°C	[17]
	Lorenz efficiency	$\eta_{Lorenz}$	0.47	-	[1]

For systems where several heat pumps are connected in series, as is the case for DH plants, the COP for the system is calculated from the Lorenz COP rather than the Carnot COP. The

Lorentz COP uses the log mean temperatures,  $T_{lm}$ , of the in- and outflow temperatures,  $T_{in}$  and  $T_{out}$ , to calculate the maximum COP for a given system, as seen in Eq. (10). Depending on the system, the source is either the air or ground, while the sink is the water circulated in the district heating grid.

$$COP_{Lorenz} = \frac{T_{lm,sink}}{T_{lm,sink} - T_{lm,source}}, \quad \text{Where } T_{lm} = \frac{T_{in} - T_{out}}{\ln\left(\frac{T_{in}}{T_{out}}\right)} \quad (10)$$

The real COP of the system is found from the Lorenz efficiency given in [1], this efficiency is used to account for the mechanical and thermal losses in the system.

$$COP_{real} = COP_{Lorenz} \cdot \eta_{Lorenz} = COP_{Lorenz} \cdot 0.47 \quad (11)$$

The nameplate efficiency, given in [1], includes losses due to defrosting and fans. Therefore, the COP of the 35°C/70°C system is calculated at -1°C to find the system efficiency when these losses are included.

First, the COP without energy consumption for defrosting and auxiliary electricity consumption is calculated in Eq. (12).

$$COP_{35^\circ C/70^\circ C} = \frac{T_{lm,sink}}{T_{lm,sink} - T_{lm,source}} \cdot \eta_{Lorenz} = 2.75 \quad (12)$$

Then the system efficiency,  $\eta_{system}$ , is calculated as the ratio between the nameplate COP and the heat pump COP as Eq. (13).

$$\eta_{system} = \frac{COP_{nameplate}}{COP_{35^\circ C/70^\circ C}} = \frac{2.55}{2.75} = 0.929 \quad (13)$$

The nameplate efficiency for the 40°C/80°C system is then calculated from the Lorenz COP, and the Lorenz and system efficiency in Eq. (14).

$$COP_{40^\circ C/80^\circ C} = \frac{T_{lm,sink}}{T_{lm,sink} - T_{lm,source}} \cdot \eta_{Lorenz} \cdot \eta_{system} = 2.30 \quad (14)$$

The varying COP is found in the same way from the average daily temperatures. The average daily temperatures, rather than the hourly, are used because [1] assumes that smaller heat pumps under 1.5 MW are designed with a secondary glycol circuit between the evaporator and the air coolers. This circuit acts as a buffer, smoothing out the temperature fluctuations throughout the day. The heat storage included in the layout can also help balance the intraday fluctuations. The average daily temperatures are found from [9], and the resulting varying and average COP can be seen in Fig. 9, along with the nameplate COP, which is a conservative assumption, to account for the low efficiency in the colder months.

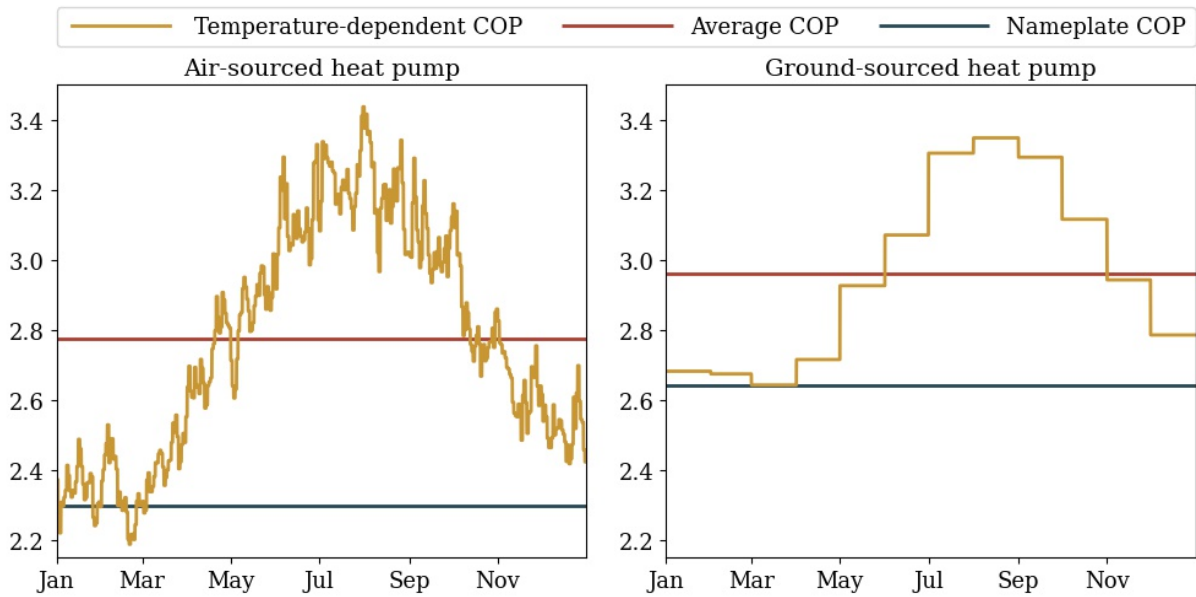


**Figure 9:** COP for the air- and ground-sourced heat pumps in 2018. The actual COP is considerably higher than the nameplate COP for most of the year.

#### *COP for ground-sourced heat pump*

The COP for the GSHP is found from the same formulas. Here the system efficiency accounting for defrosting and auxiliary electricity consumption in the ASHP is set to 1, as defrosting is irrelevant for the GSHP.

The Lorenz efficiency is assumed to be the same as for the ASHP, and the source temperature used is the monthly ground temperature 1 meter below the surface from [3]. The resulting COP can be seen in Fig. 9 where the nameplate COP is set to the lowest monthly COP.

#### *Minimum working temperature for ASHP*

As seen in Fig. 9, the COP for an air sourced heat pump decreases with the air temperature and starting at  $-10^{\circ}\text{C}$ , the heat pumps ability to efficiently extract heat starts to decline [24]. If the temperature drops below this threshold for several days, the heat pump will not be producing at the rated efficiency, and the system will depend on the resistive heater and the hot water tank to cover the total heat demand. Since the modelled temperatures used for the optimisations are not precisely capturing the extreme temperatures, the measured temperatures from DMI are examined in Fig. 10. Here it can be seen that the lowest measured temperature was only below  $-10^{\circ}\text{C}$  for four days in 2012, but the average daily temperature was never below  $-10^{\circ}\text{C}$  for any of these four days. Since the lowest measured temperature on Samsø in the last ten years,  $-11.9^{\circ}\text{C}$ , still gives a COP of 1.96, and given that safety coefficients will be applied to the optimisation results, the minimum working temperature for an air-sourced HP is not considered an issue.

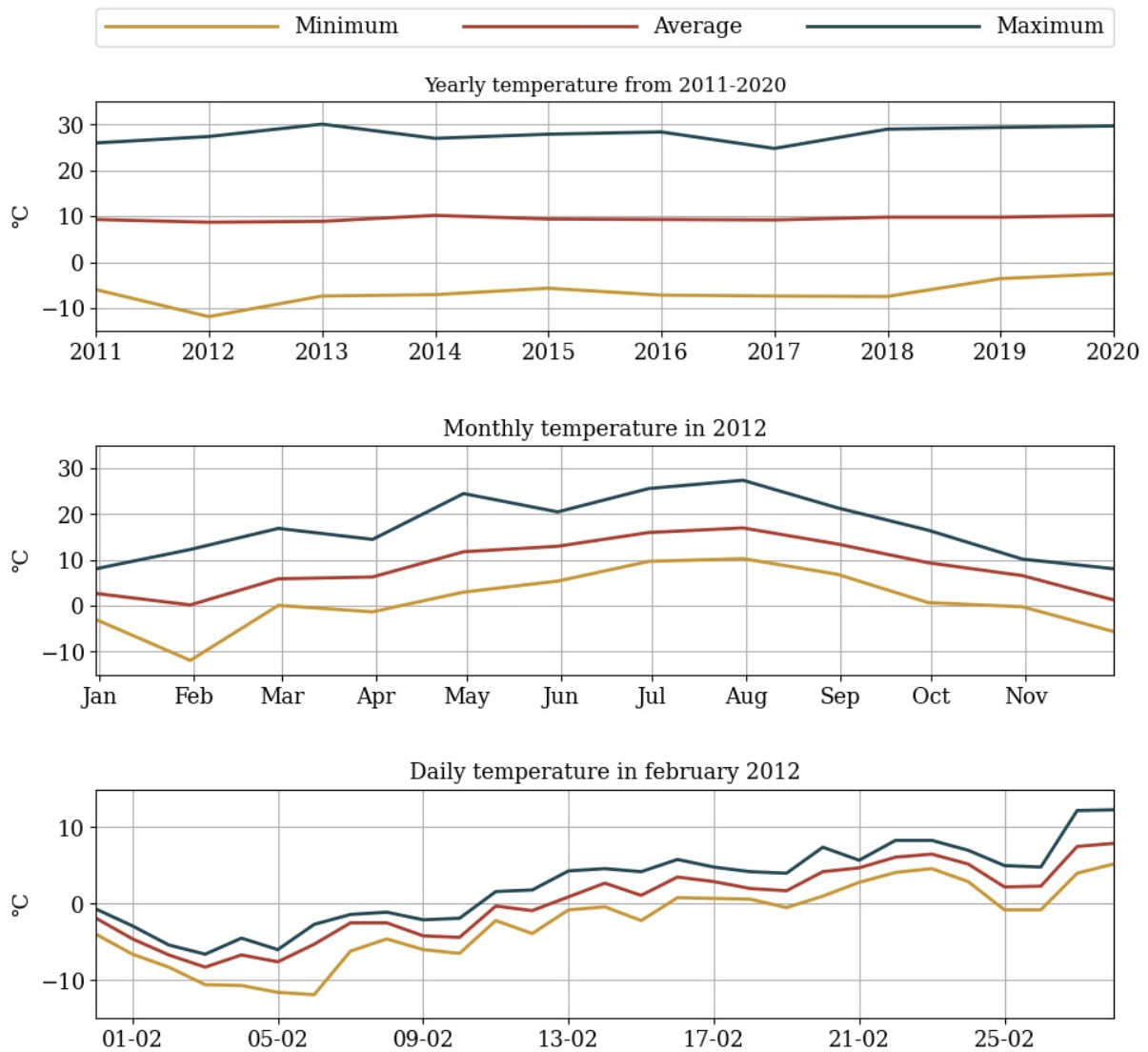


**Figure 10:** Historical measured temperature on Samsø.

## 2.5 HYDROGEN

This section gives an overview of the components needed for hydrogen storage and the cost associated with them. In Fig. 11 the components can be seen. Here hydrogen is produced with an electrolyser, which uses electricity to split water into hydrogen and oxygen. The produced hydrogen is stored in pressurised steel tanks. When electricity production is low, the hydrogen can be converted back into electricity in a fuel cell.

The assumed costs for the components can be seen in Table 14 and Table 15.

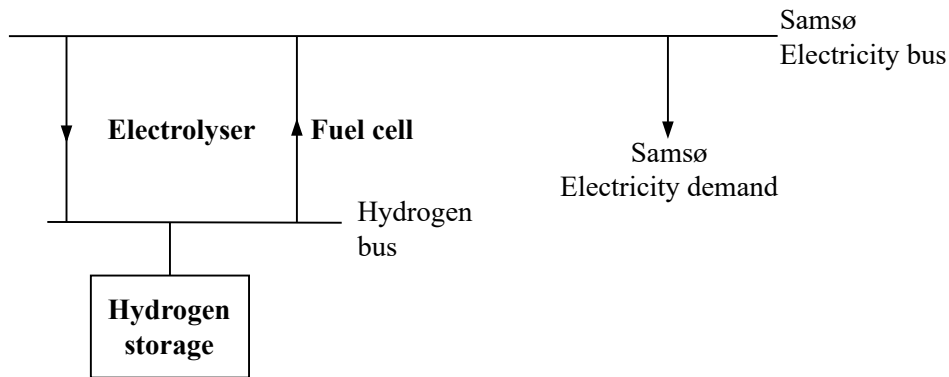


**Figure 11:** Model overview for hydrogen storage. The components, which are optimised, are marked in bold.

**Table 14:** Data for renewable energy conversion technologies. Assumptions are taken from the Danish Energy Agency (DEA) Technology Database, [1] and [8].

	<b>Electrolyser</b>	<b>Fuel cell</b>	Unit
Typical rating	10	10	MW
Efficiency	63.6	50	%
District heating output	14	-	%
Lifetime	25	10	Years
Capital cost	0.60	1.3	2015-M€ /MW
Cost uncertainty	±33.3	+23.1 -15.4	%
Fixed O&M	30,000	65,000	2015-€ /MW/year

## 2.6 TRANSPORT

When the residents on Samsø, especially in the private transport sector, start trading in their Internal Combustion Engine (ICE) vehicles for plug-in hybrids and battery electric vehicles (BEV), the energy demand on the island will increase. However, the battery capacity in the vehicles can also help balance the fluctuation of the VRES.

In this section, the energy demand and the storage and power capacity of the transport sector are established.

As Samsø is a small island with a length 27 kilometres, making it ideal for BEV's. Consequently, it is assumed that all private cars on the island will be replaced by BEV's in the future. The size

**Table 15:** Data for hydrogen storage. Assumptions are taken from catalogues published by the Danish Energy Agency (DEA) Technology Database [6].

	Hydrogen storage	Unit
Energy storage capacity for one unit	16.7	MWh
Lifetime	25	years
Capital cost	57,000	2015-€ /MWh
Fixed O&M	600	2015-€ /MWh/year

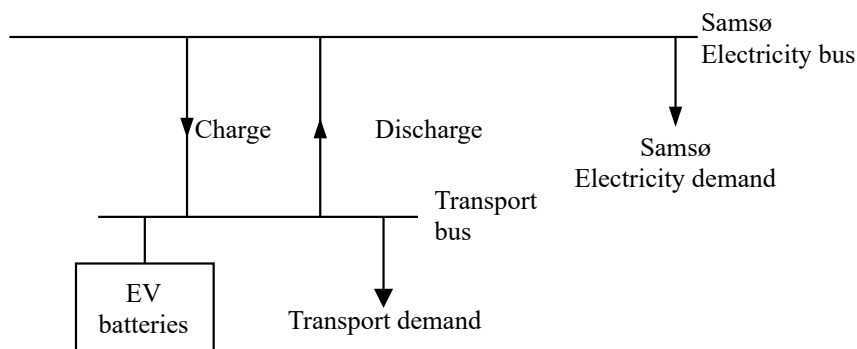


**Figure 12:** Model overview for transport sector.

of the island also reduces the transport demand. Therefore, the transport demand on Samsø is assumed to be 70% of the average demand in Denmark.

In Fig. 12 the transport model can be seen. Here the electricity sector is linked to the transport sector by a charging and a discharging link. The hourly transport demand is found from the time-series provided by [23], which defines the fraction of vehicles not in use. When in use, the vehicles are assumed to have a constant demand, such that the annual use matches the annual demand.

When the vehicles are not used, they are assumed to be connected to the grid. Here all connected vehicles available for charge, while 25% of the connected vehicle can also discharge, to provide vehicle-to-grid services. The daily profile for the transport sector can be seen in Fig. 13.

The energy consumption for the BEV's, their battery capacity, and charging capacity and efficiency are taken from [22] and can be seen in Table 16. The annual transport demand and the total storage and charging capacity are calculated below and summed up in Table 17.

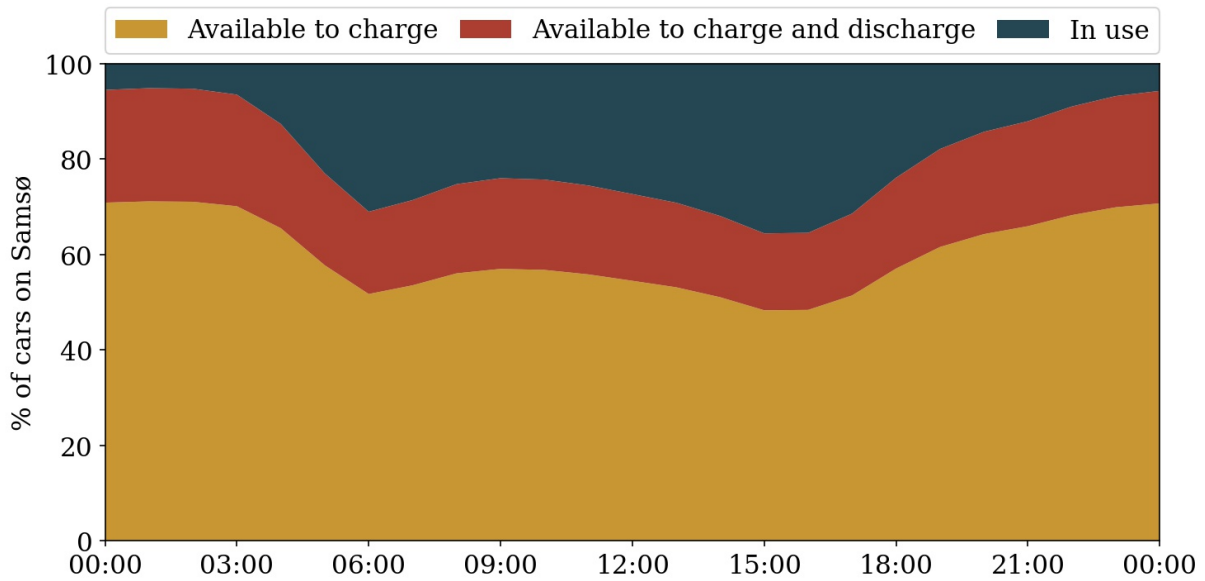


**Figure 13:** Daily profile for the transport demand. When the vehicle is not in use, it is assumed to be connected to the grid. All connected cars are available for charge, 25% are also available for discharge.

**Table 16:** Data for the BEV's included in the model

Energy consumption	Battery capacity	Charging capacity	Charging efficiency
0.2 kWh/km	50 kWh/vehicle	11 kW/vehicle	90%

When excluding commercial transport, the daily vehicle mileage was 23.6 km/person/day in 2019 [25]. This gives a total mileage for Samsø of 60,900 km/day, as calculated in Eq. (15)

$$\text{Daily transport demand} = 23.6 \text{ km/person/day} \cdot 3,684 \text{ residents} \cdot 70\% = 60,860 \text{ km/day} \quad (15)$$

With an energy demand of 0.2 kWh/km [22], the annual transport demand can be calculated from Eq. (16) as 4.4 GWh.

$$\text{Annual transport demand} = \frac{60,860 \text{ km/day}}{365 \text{ days/year}} \cdot 0.2 \text{ kWh/km} = 4.4 \text{ GWh/year} \quad (16)$$

In Denmark, there are 447 cars per 1,000 people [26], and assuming this statistic holds for Samsø, and that an average battery capacity of 50 kWh, this results in a total storage capacity in the transport sector of 82 MWh, as calculated in Eq. (17).

$$\text{Total battery capacity} = \frac{447 \text{ vehicles}}{1,000 \text{ people}} \cdot 3,684 \text{ residents} \cdot 50 \text{ kWh/vehicle} = 82 \text{ MWh} \quad (17)$$

With an average charging capacity for the vehicles of 11 kW, the total charging capacity is 18 MW, as calculated in Eq. (18).

$$\text{Total charging capacity} = \frac{447 \text{ vehicles}}{1,000 \text{ people}} \cdot 3,684 \text{ residents} \cdot 11 \text{ kW/vehicle} = 18 \text{ MW} \quad (18)$$

The transport storage is required to have a minimum filling level of 75% each morning at 5 am, such that the vehicles are charged and ready to get the residents to work on time.

**Table 17:** Data for the BEV's included in the model

Transport demand	Total battery capacity	Total charging capacity
4.4 GWh/year	82 MWh	18 MW

# 3 BALLEEN-BRUNDBY DISTRICT HEATING PLANT

Ballen-Brundby district heating plant is modelled in PyPSA as described in Section 2.4.1 and the results will be analysed as seen in Fig. 14.

First, an initial PyPSA model is calculated from data for 2018. Then a sensitivity analysis is done to determine how sensitive the capacities and costs are to various changes in input. From this sensitivity analysis, the recommended capacities are calculated for both an ASHP and a GSHP, and the costs are calculated for these systems, with and without dispatch optimisation. Finally, the section will be concluded with a discussion and a comparison to the analysis done by Østergaard et al. in [4].

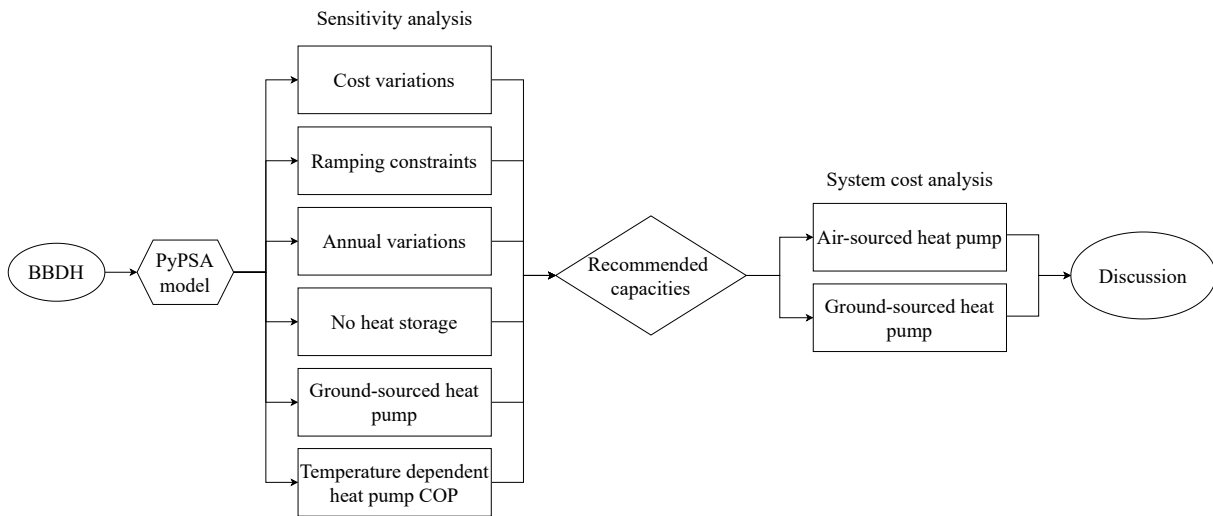


**Figure 14:** Flowchart for the analysis of Ballen-Brundby district heating plant.

## 3.1 INITIAL RESULTS

The initial system consists of a 0.84 MW ASHP which produces 90% of the required annual heat output for the plant, while the 0.40 MW resistive heater helps cover the peak load in the winter. The system has an 11 MWh heat storage that balances the on/off regulation of both the heat pump and the resistive heater seen in Fig. 15. Here it is clear that when the required heat

output is lower than the system capacity, either the heat pump or the resistive heater shuts off once or twice a day, at times corresponding to the higher electricity prices in the morning and evening.

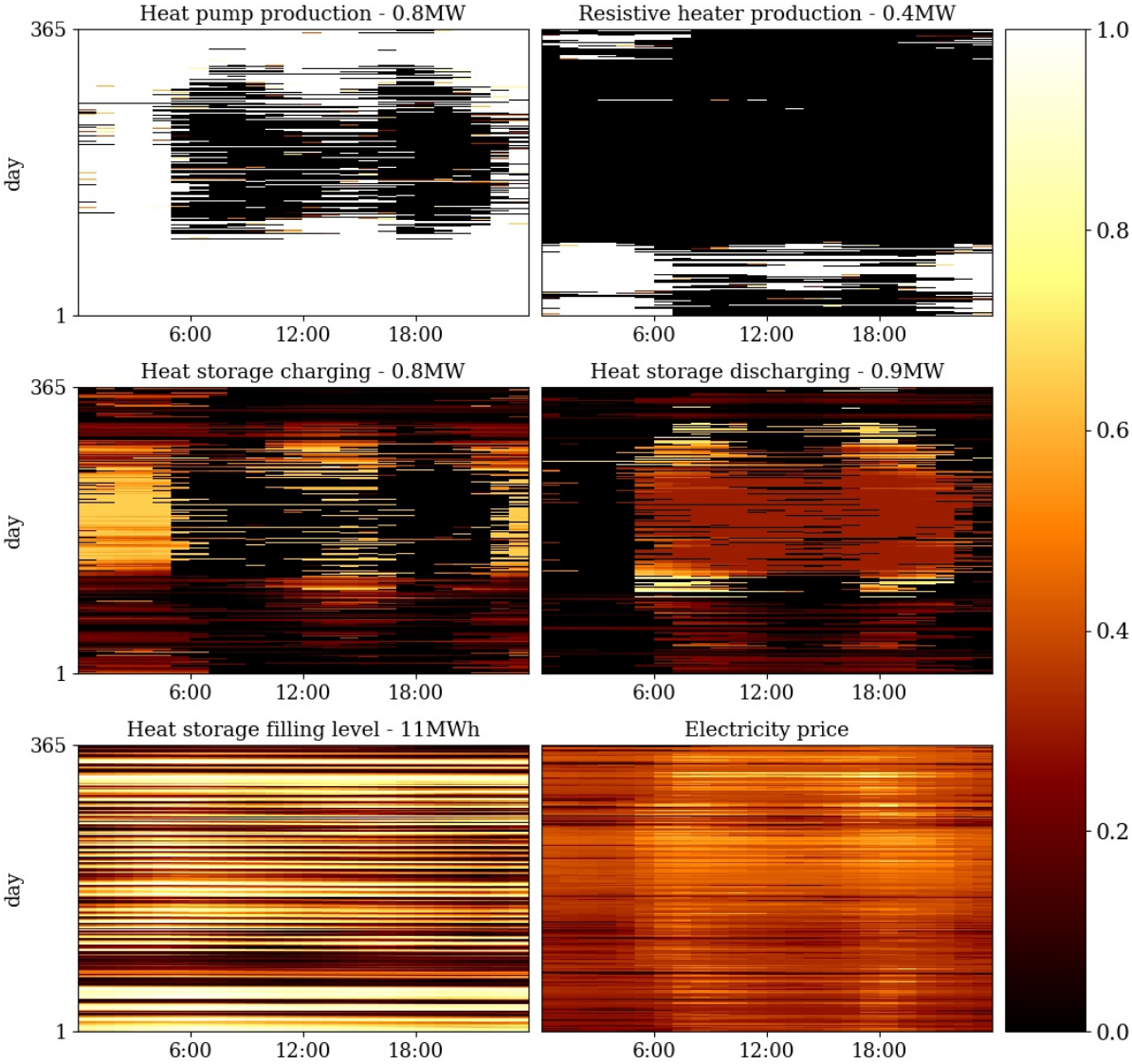


**Figure 15:** Heat production, electricity price, and charging, discharging and filling level for heat storage throughout the year in 2018.

There is no clear seasonal profile for the heat storage. Furthermore, the storage is large enough that the daily discharge in the morning and evening are not seen in the filling level, but not large enough that the storage is used to balance the seasonal profile of the heat demand.

From Fig. 16 it can be seen that the heat pump, on average, shuts off around 300 times a year. It is also clear that the regulation method for both the heat pump and the resistive heater is primarily on/off, which is also seen from the duration curves in Fig. 18a. This is only

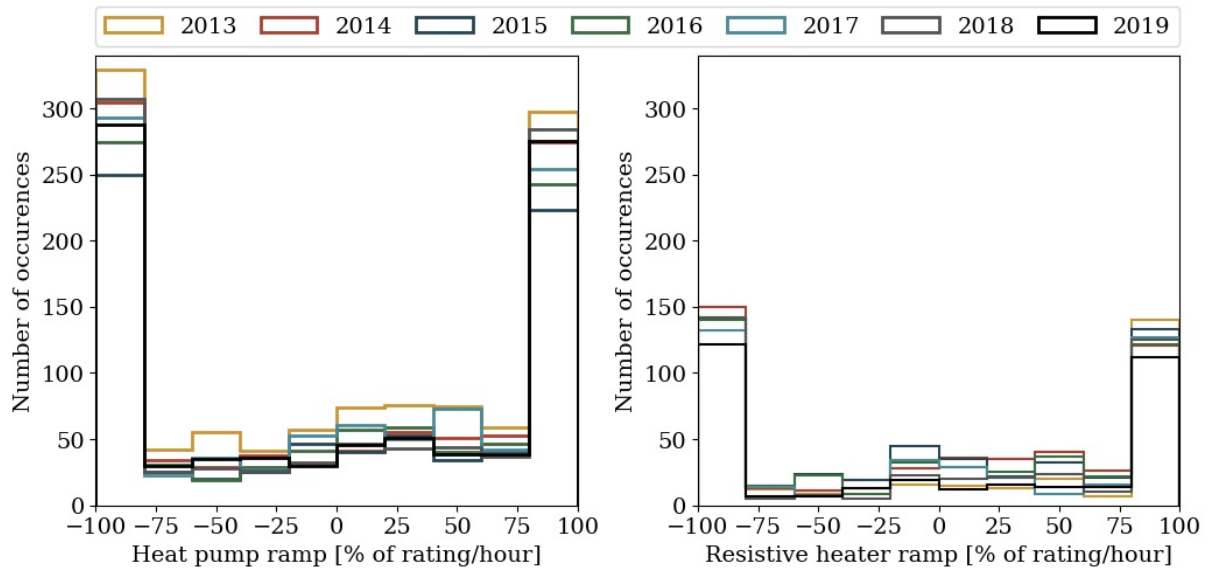


**Figure 16:** Ramps for heat pump and resistive heater the years 2013-2019.

possible because of the storage, as the heat production is frequently larger and smaller than the required output of the plant, as seen in Fig. 17.

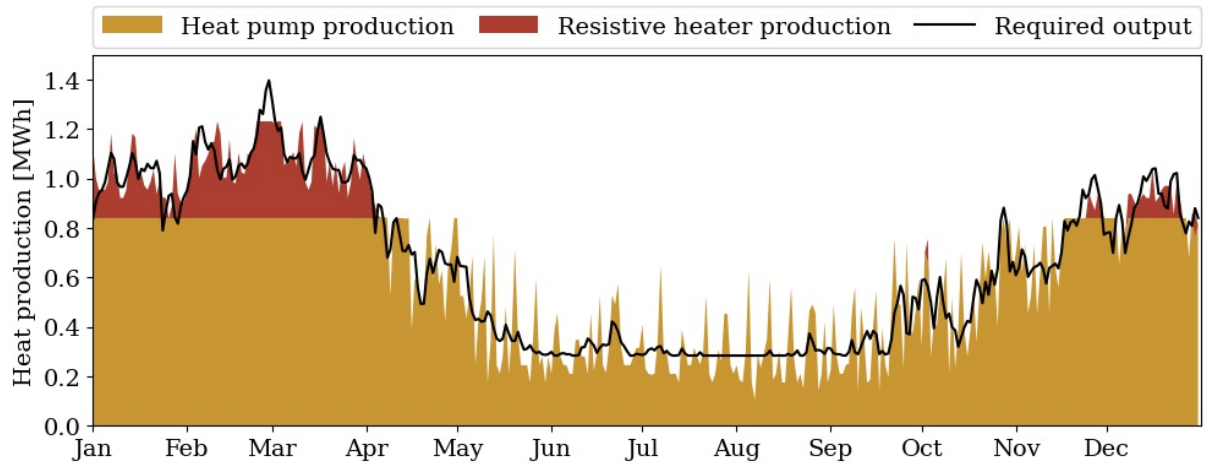
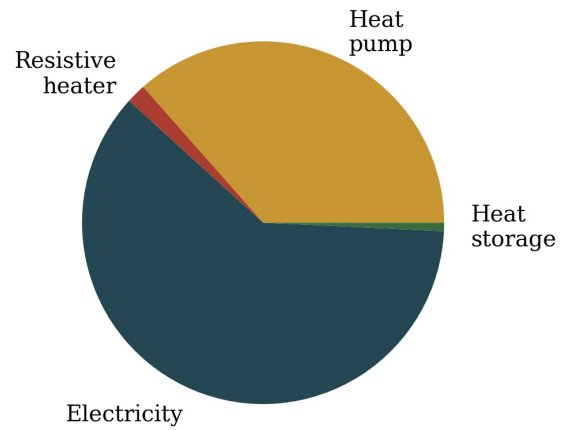
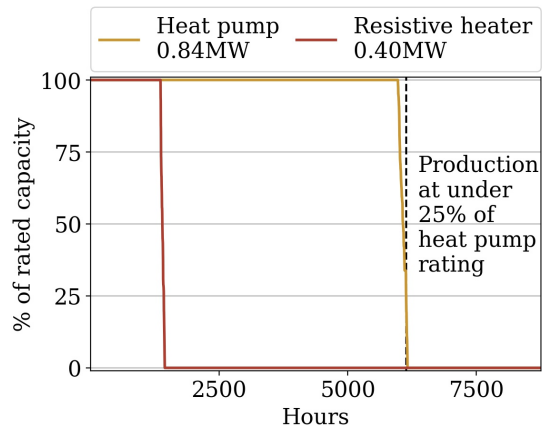


**Figure 17:** Average daily heat production by source and required heat output in 2018. Storage is used to balance mismatch between heat production and the required output.

While the heat pump is limited by the given minimum load of 25% of the rated capacity from [1], it only operates below this limit for an average of 33 hours of the year as indicated in the duration curve for 2019 seen in Fig. 18a. Therefore it is not considered necessary to impose a minimum load constraint on the system since it would completely prevent the heat pump from switching off.



(a) Duration curves for heat pump and resistive heater in 2018, the resistive heater is used around 1,500 hours of the year while the heat pump is used around 6,100 hours.

(b) The total annual costs for the system, when optimised for the year 2018, is 0.36 M€, with the costs split mainly between the heat pump and electricity.

**Figure 18:** Duration curves and average daily heat production for BBDH in 2018.

When the model is optimised for 2018, the annual system cost is 0.36 M€. This is mainly spent on the heat pump and electricity, with only 2.5% of the annual system cost spend on the resistive heater and storage combined as seen in Fig. 18b. This also means that an increase of either of these components would be a cheap way to ensure that the plant can always meet the required output, even during maintenance or if the heat pump has a low efficiency on an exceptionally cold day.

### 3.2 SENSITIVITY ANALYSIS

A sensitivity analysis is carried out to assess how much the capacities and costs vary when subjected to external variations. First, it is examined how different scenarios affect the optimal capacities found for 2018. Then several of these models are optimised for the years 2013-2019 to see how the models compare to each other and how sensitive they are to annual variations.

#### 3.2.1 Cost variations

As the component costs found from in [1] and [6] have some uncertainties connected to them, the model is run for costs varying from the lower to the upper range for the capital cost of each component. In addition, the layout is optimised for variations in the electricity spot prices, where the cost variation is calculated as the range of the average yearly electricity price for the years 2013-2019.

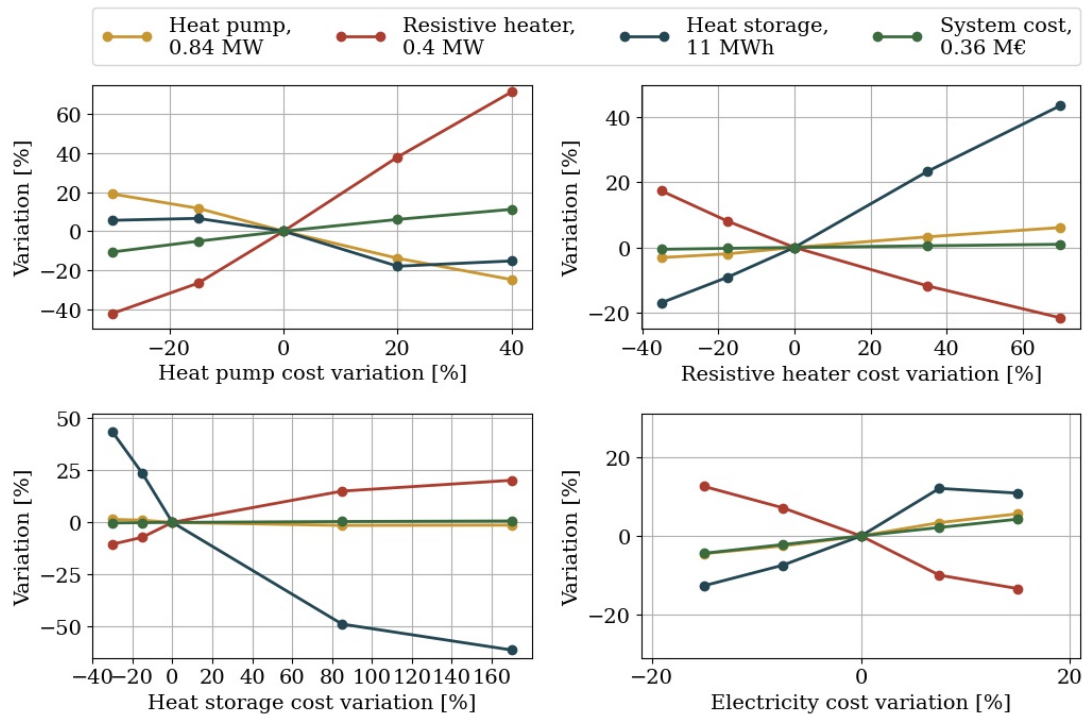


**Figure 19:** Sensitivity to cost variations based on values for 2018. To provide a scale for the different cost variations and their impact on the capacities and the annual system cost, the grid lines in all figures have a distance of 20%. The initial values can be seen in the legend.

The result of this analysis can be seen in Fig. 19, where it is clear that the change in capital costs of either the resistive heater or the heat storage will affect the other, as they both have the function of smoothing the peak loads. Nevertheless, even though they have significant cost uncertainties, neither have much influence on the optimal heat pump capacity or the resulting system cost, as they both have relatively low associated costs as seen in Fig. 18b. As such, even a 70% increase in the capital cost for the resistive heater only increases the heat pump capacity by 6%.

The maximum variation in capital cost for the heat pump will affect the resulting system cost with  $\pm 10\%$ . This, of course, is because the heat pump cost contributes significantly to the annual system cost. However, when the heat pump is downsized in favour of the resistive heater, the electricity cost increases, as the efficiency for the resistive heater is less than 40% of the heat pump COP.

The high heat pump COP also causes the system to reduce resistive heater capacity favouring the heat pump when the electricity costs are increased. The heat storage is also increased for higher electricity prices to better balance peak loads and electricity prices.

Removing the discount rate yields results similar to reducing the component capital costs, as the annualised cost no longer includes inflation. This results in a reduction in annualised capital costs of 21%. As the variation in capital costs for the resistive heater and the heat storage mainly affected each other, the result is similar to the reduced capital cost for the heat pump. The result is an increase in heat pump and storage capacity, a reduced resistive heater capacity, and a lower system cost.

### 3.2.2 Ramping constraints

Heat pumps have a high level of adaptability compared to the current straw boiler, but the on/off regulation seen in the summer months in Fig. 15 can wear on the components. Therefore, it is examined how the system cost and optimal capacities are impacted when the flexibility of the heat pump is decreased. The ramping constraints imposed on the system limit the change in heat pump production from one hour to the next, reducing the heat pump’s flexibility.

The resulting HP production is shown in Fig. 20, where it can be seen that the HP still tries to adapt to the increase in electricity prices in the morning and evening, but, due to the ramping constraint, the summer heat production is spread out over the day rather than mainly limited to the nighttime.

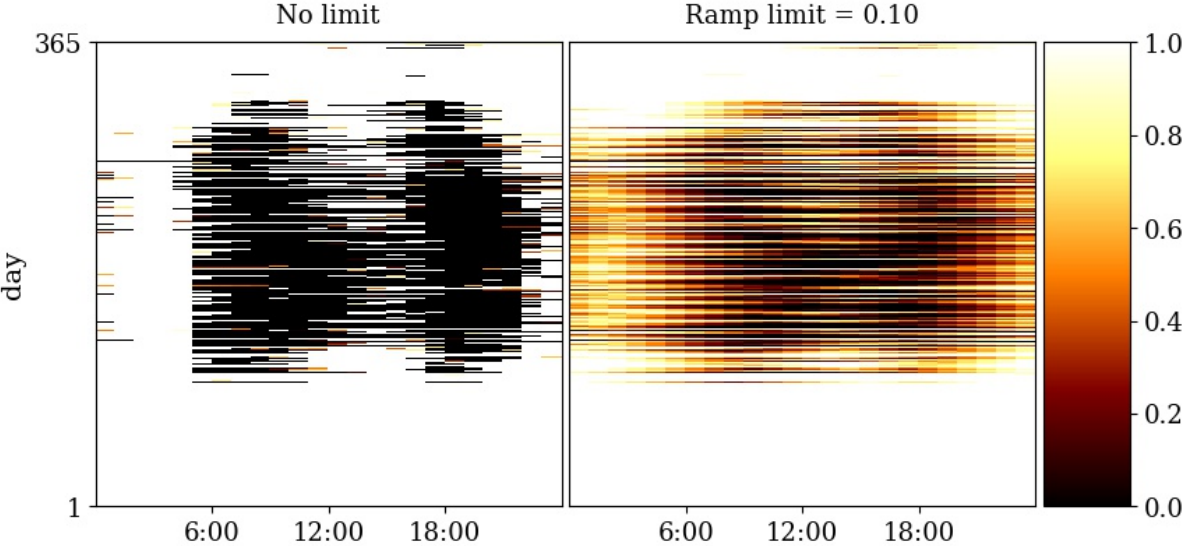


**Figure 20:** Comparison of heat pump production with a ramping limit of 0.10 and without ramping limit.

In Fig. 21 the capacities’ sensitivity to ramping constraints are plotted, and it is clear that the limitation of the HP’s flexibility leads to an increase in the need for heat storage to provide this flexibility. Therefore, it is also to be expected that the HP capacity decreases slightly as

the constraints imposed on it increase. However, it is not immediately clear why the resistive heater capacity also decreases. An explanation for this is the required increase in heat storage capacity. As both of these components balance peak loads, the increase in storage capacity helps balance a larger part of the winter peak load, otherwise covered by the resistive heater.

As ramping constraints on the HP only significantly affect the storage capacity, which contributes very little to the annual expenses, any ramping constraints should be imposed on the system rather than the model. If any ramping constraints are imposed on the system, considerations should be made regarding the chosen size of the heat storage.

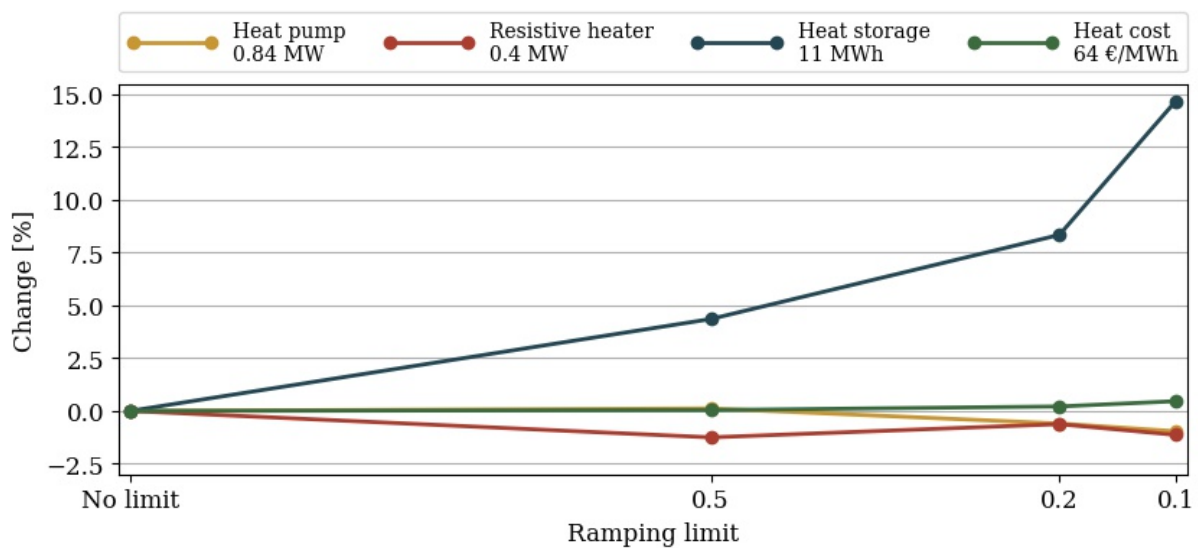


**Figure 21:** Sensitivity to increased ramping constraints, based on values for 2018. The initial values can be seen in the legend.

### 3.2.3 Annual variations

As the heat demand and electricity prices vary from year to year, the model is run for 2013-2019 to see how sensitive the optimal capacities are to these variations. The result of this analysis can be seen in Table 18. The heat pump capacity, which makes up most of the investment cost, has an average capacity of 0.78 MW, with a variation of about  $\pm 10\%$ , while the heat pump and heat storage vary by up to 28% throughout the seven years. The resulting system cost variations are comparable to that of the heat pump with a maximum variation of 11%.

**Table 18:** Resulting capacities and costs for the model run for the years 2013-2019

	Minimum	Average	Maximum	Unit
Heat pump	0.70	0.78	0.84	MW
Resistive heater	0.29	0.36	0.44	MW
Heat storage	6.74	9.34	11.4	MWh
Yearly heat production	0.51	0.55	0.56	GWh
System cost	0.29	0.32	0.36	M€

### 3.2.4 Varying COP

Changing the COP of the ASHP to depend on the daily temperatures leads to a decrease in the HP capacity and an increase in resistive heater capacity as seen in Table 19. This is due to the seasonal profile of the COP, which increases in the summer, where the heat demand is low and decreases in the winter when the heating demand is largest. Another factor, which reduces the heat pump capacity, is the relatively conservative definition of the heat pump COP. As seen in Fig. 9, the actual COP is significantly higher than the nameplate COP for the majority of the year.

The smaller heat pump leads to a lower system cost, as the decrease in investment cost for the heat pump more than outweighs the increase in electricity use for the resistive heater.

**Table 19:** Comparison between resulting capacities and costs for constant and varying COP calculated from data for 2018.

	ASHP - Constant COP	ASHP -Varying COP	Change [%]
Heat pump [MW]	0.84	0.80	-5.3
Resistive heater [MW]	0.40	0.44	12.3
Heat storage [MWh]	11.4	10.5	-7.76
Annual cost [M€]	0.36	0.33	-8.5

### 3.2.5 No heat storage

At the request of the BBDH board, a model without storage is set up. The results of this can be seen in Table 20. Eliminating the storage removes the system's ability to balance the heat production to the electricity prices. Therefore, the system requires larger capacities to cover

peak loads, especially for the resistive heater, which increases by almost 50%. Nevertheless, the system cost has a surprisingly slight increase of 1.2%, suggesting that balancing the electricity price does not significantly impact the cost, even though electricity makes up around 60% of the total system cost. This model is also run with the ramping constraints from Section 3.2.2, which have no impact on the capacities as the HP never shuts off and the maximum change in the required heat output from one hour to the next only corresponds to 10.5% of the heat pump capacity.

**Table 20:** Comparison between resulting capacities and costs for ASHP with and without storage.

	ASHP - Constant COP	ASHP - No storage	Change [%]
Heat pump [MW]	0.84	0.88	4.8
Resistive heater [MW]	0.40	0.58	47
Heat storage [MWh]	11.4	0.00	-100
Annual cost [M€]	0.36	0.36	1.2

### 3.2.6 Ground-sourced heat pump

As noise pollution can be an issue for the ASHP, the model is also run for a GSHP system, the result of which can be seen in Table 21. An added benefit of a GSHP is that the source temperature is less fluctuating than air, and the temperatures are higher in the winter when the heat demand is highest. While the GSHP has a higher COP than the ASHP, the capital cost is also higher, causing a decrease in HP capacity of 25% and an increase in resistive heater capacity of 60%. Even with the decrease in HP capacity and the larger COP in winter, the system cost increases by 14%.

**Table 21:** Comparison between resulting capacities and costs for air-sourced and ground-sourced heat pumps with varying COP.

	ASHP - Varying COP	GSHP - varying COP	Change [%]
Heat pump [MW]	0.80	0.59	-25
Resistive heater [MW]	0.44	0.71	60
Heat storage [MWh]	10.5	10.5	-0.7
Annual cost [M€]	0.33	0.38	14

The noise pollution needs to be examined before selecting the final system to ensure that the issue is large enough to warrant this cost increase.

### 3.2.7 Comparison between sensitivities

In Fig. 22 the result of different models run for the years 2013-2019 is shown. From the figure, it is clear that when the heat storage is included, its capacity varies very little from model to model. The same is true for the resistive heater when going from constant COP to temperature dependant COP, but the resistive heater more than doubles to make up for the missing heat storage in the model without storage.

For both the ASHP and the GSHP, the annual system cost is lower for the models with varying COP. One reason is the smaller heat pump, but another reason is the decrease in electricity cost due to the higher COP.

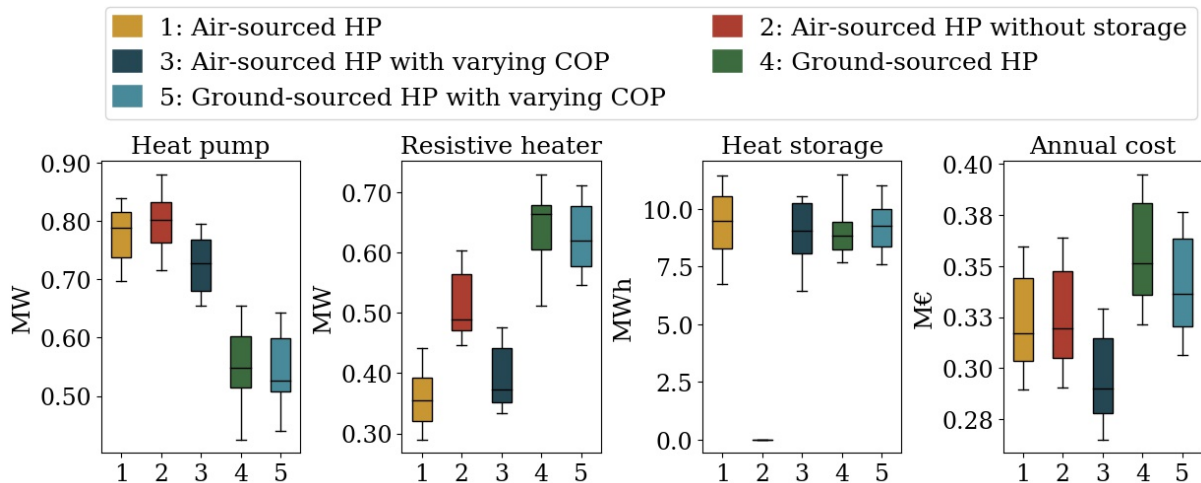


**Figure 22:** Resulting capacities and annual costs for various models. In model 1-3 the system has an air-sourced heat pump, while the heat pump in model 4 and 5 is ground-sourced.

### 3.3 RECOMMENDED SYSTEM AND COST ANALYSIS

In this section, the recommended capacities for the system are given for both an ASHP and a GSHP system. The model is run for both cases with and without electricity price optimisation.

The recommended capacities are found from the largest optimal capacities found for the two models with varying COP run for 2013-2019. The varying COP better reflects the reality than the constant COP, and the largest values for each component are chosen as an added

safety measure at the request of the board for BBDH. They also require that the system can support a continuous output of 2 MWh from direct heat production.

A safety factor of 1.5 is chosen for the heat pump, while the safety factor for the resistive heater and the heat storage is chosen to be 2. This is chosen because both the resistive heater and the heat storage have modest capital costs compared to the HP, so increasing their size is a cheap way to ensure that the system can handle peak loads above historical levels. The safety factor of 1.5 for the heat pump is used to secure the system against uncertainties in the heat demand modelling. The resulting capacities can be seen in Table 22.

**Table 22:** Recommended capacities for the systems with air-sourced and ground-sourced heat pumps. Capacities are calculated with a safety factor of 1.5 for the heat pump and 2 for the cheaper resistive heater and heat storage.

	Air-sourced	Ground-sourced	Unit
Heat pump	1.2	1.0	MW <sub>heat</sub>
Resistive heater	1.0	1.4	MW
Heat storage	21	22	MWh

When these models are run for 2013-2019, they result in a maximum annual system cost of 0.37 M€ with an ASHP and 0.42 M€ with a GSHP. The maximum heat production cost for these systems are 32 €/MWh for the ASHP and 31 €/MWh for the GSHP.

Removing the systems ability to adapt the heat production to the electricity prices leads to the cost increases seen in Fig. 23. For the years 2013-2019, the maximum increase in electricity cost is 8.5% and 7% for the ASHP and GSHP, respectively. However, when looking at the annual cost, the increase is around 4% for the ASHP and 2.5% for the GSHP, corresponding to 14,000€ and 11,000€ respectively. The maximum production cost increases to 35 €/MWh for the ASHP and 33 €/MWh for the GSHP.

In the actual operation of a system without electricity optimisation, this cost increase might be more significant since the daily profile of the hot water demand is not included in the model, and these morning peaks correspond to the morning peak in electricity cost.

### 3.4 DISCUSSION

In [4] Østergaard et al. examine the operation of the BBDH plant by using EnergyPRO to optimise the operation for set capacities. Varying the heat pump and heat storage capacities

and evaluating the results leads to conclusions on optimal capacities for each of these components, specifically a heat storage capacity between 10-15 MWh and a HP capacity of  $0.5\text{MW}_{\text{el}}$ . Assuming a nameplate COP that corresponds to the one calculated from information from [1], this leads to a HP capacity of  $1.15\text{MW}_{\text{thermal}}$ .

Both of these are higher than the optimal capacities found from PyPSA, which both optimises capacity and dispatch. It is worth noting that [4] includes the electricity levy in the electricity price, which on average increases the electricity price by 47%. In Fig. 19 it was seen that increasing the electricity cost resulted in larger capacities for both the HP and heat storage, so the inclusion of this levy explains why the capacities determined by [4] are higher than the ones found in this model optimised in PyPSA.

The price of direct heat production is  $35\text{€}/\text{MWh}$  when the system has an ASHP, which is the exact direct production cost as the current system [7]. The system with a GSHP has a slightly lower production cost of  $33\text{€}/\text{MWh}$ , but as determined in Section 3.2.6 choosing a GSHP over an ASHP will result in an overall cost increase of 14%.

Unlike the results from [4] it is found that the production cost of the electrified district heating plant and the reason for this is the reduced electricity fees. As most of the production cost is the electricity cost, reducing the average cost of electricity by almost a third has a significant impact on both the system and production cost.

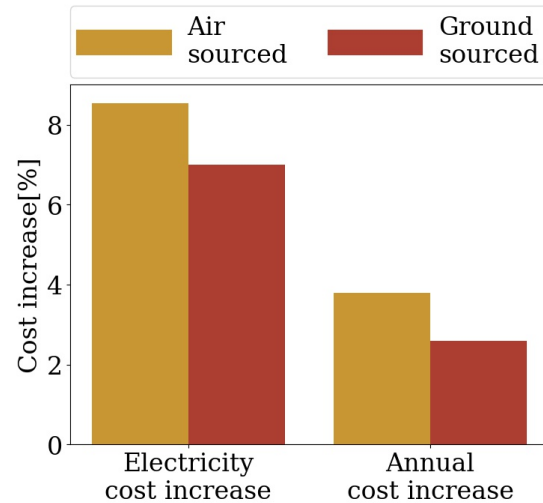


**Figure 23:** Maximum cost increases for the models run for the years 2013-2019 without electricity cost optimisation.

## 4 SAMSØ ENERGY SYSTEM

---

The energy system on Samsø is examined to determine the system dynamics, the benefit of sector coupling and the optimal renewable capacities for the island. This analysis is done in two stages. First, the VRES capacities are fixed to the current installations, and the system dynamics are examined for the current electricity sector and a coupled electricity and heating sector. This analysis attempts to answer the questions seen in Fig. 24.

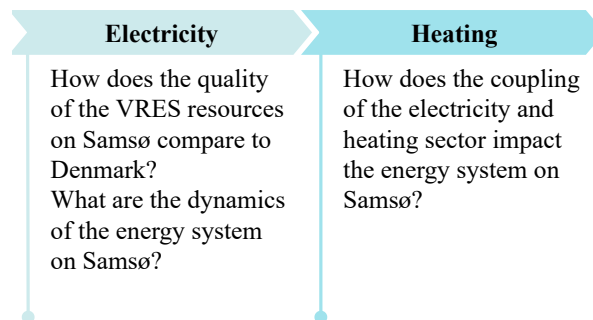


**Figure 24:** The energy system is modelled for fixed capacities to examine the dynamics of the current system and determine the impact of electrifying the district heating sector.

In the second stage, with the steps seen in Fig. 25, the capacities are allowed to expand. As the transmission capacity to DK1 is limited, it is examined if it is beneficial for the system to balance production with either hydrogen storage or an electrified transport sector.

As the cost of installing more VRES is expected to decrease towards 2050, it is also examined how lower associated costs affect the system's optimal VRES capacities. As both heat demands, electricity spot prices and capacity factors vary from year to year, average time-series have been modelled for all fluctuating inputs.

The current electricity system on Samsø can be seen in Fig. 3 and overviews of all expanded systems can be seen in Appendix C.

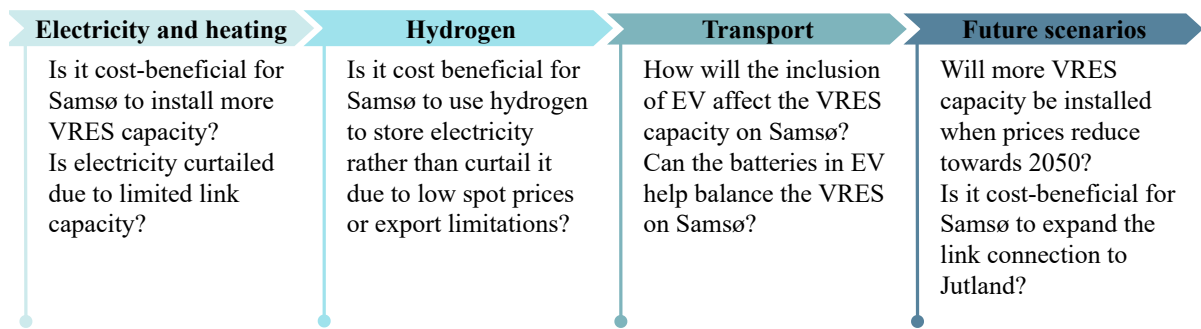


**Figure 25:** As Samsø aims to increase the VRES capacities in the future, the energy system is allowed to increase the installed capacity in this stage. Again the system is modelled in steps to see what happens as sector coupling increases. Lastly, the impact of the expected cost-reduction towards 2050 and the possibility of expanding the link to DK1 is examined.

#### 4.1 CURRENT VRES CAPACITIES

##### 4.1.1 Electricity

In this section, Samsø's VRES quality and renewable generation patterns are investigated. The dynamics of the electricity system are also examined, including the use of the link connecting Samsø with the mainland.

The quality of the renewable resources on Samsø is above the average for Denmark as seen in Fig. 27. Wind production has an average annual capacity factor 9% higher than the national average, and the solar capacity is 15% higher than the average.

When looking at the Fourier power spectrum in Fig. 26 it is clear that the dominating frequency for wind is the annual variation. This variation is also seen in Fig. 27, where the capacity factor for wind is higher in the winter than in the summer. While wind also shows weekly and monthly patterns, these are not as dominating as the annual frequency.

Solar PV also has an annual frequency, which is very evident in Fig. 27. However, solar production is dominated by the diurnal frequency, where production occurs during the day, and ceases between sunset and sunrise. The frequency around 12 hours shows the daily profile of solar production, with peak production around noon.

As mentioned previously, Samsø is a net exporter, and this is evident in Fig. 28, where the average production on Samsø is more than five times the average electricity demand for the island. This electricity production mainly comes from wind, with solar contributing very little, as the installed capacity is less than 4% of the installed renewable capacity on Samsø.

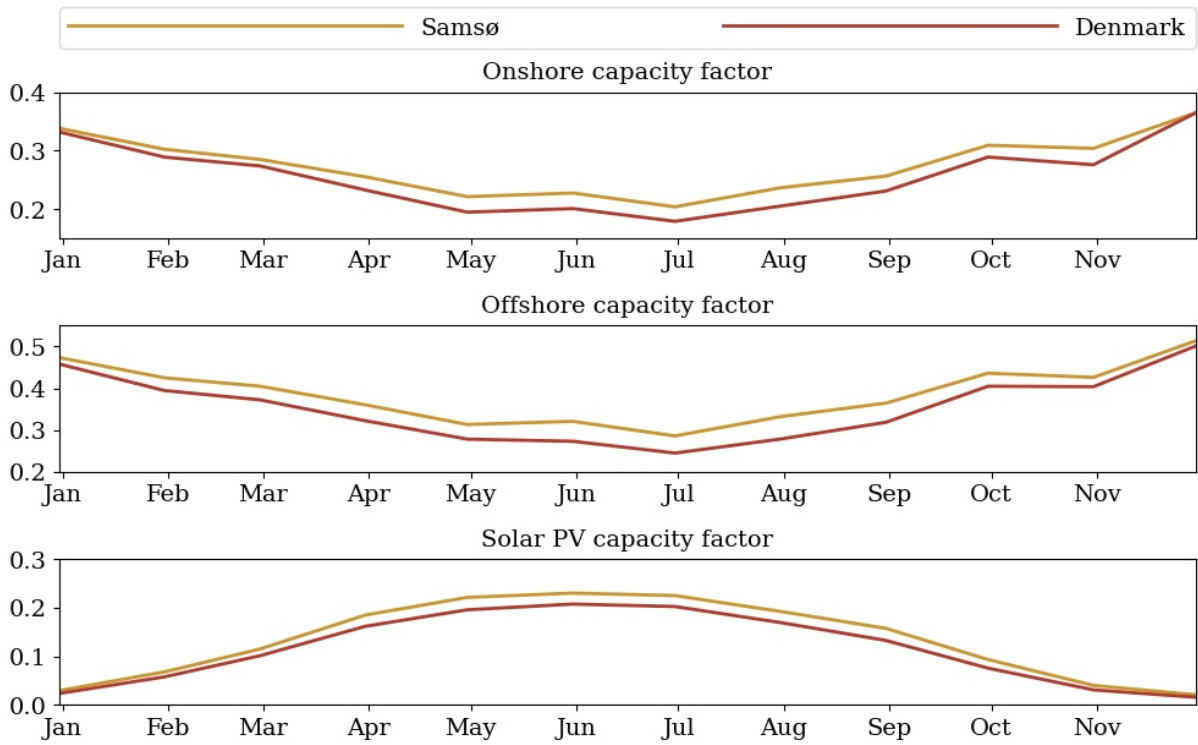


**Figure 27:** Average monthly capacity factors for Samsø and Denmark. The capacity factors on Samsø are consistently higher than the average capacity factor across Denmark.

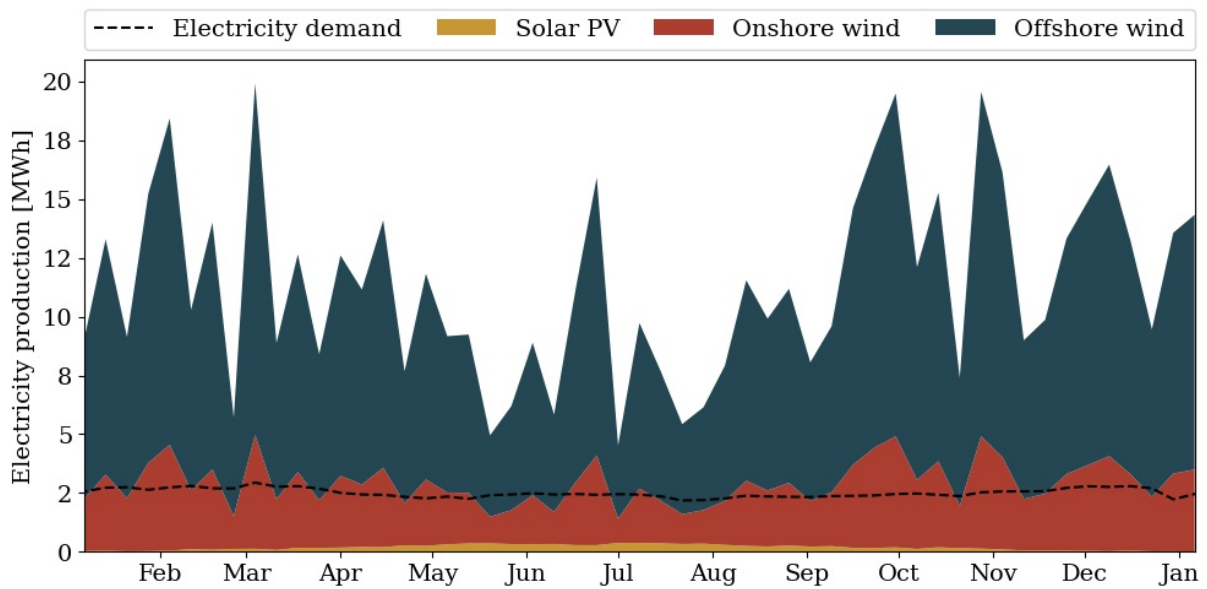


**Figure 28:** Average weekly electricity generation and demand on Samsø. The annual renewable generation on Samsø is six times larger than the annual electricity demand.

The modelled electricity demand is based on the electricity demand in DK1, and the population peak during the tourism season in the summer months is therefore not seen. As this will likely increase the actual electricity demand, it could be beneficial to install more solar PV, so the annual profile of electricity production better matches the expected actual demand on the island.

While the link to DK1 is mainly used for export, import is occasionally necessary to balance the fluctuation of the electricity production, as see in Fig. 29. In 2018 only 1.7% of the annual link flow was due to import, but this still covered 4% of the annual electricity demand on Samsø. However, the exclusion of the population increased during the summer might impact the ratio between export and import, as the primary electricity production on Samsø comes from wind production, which is lower in summer than in winter.

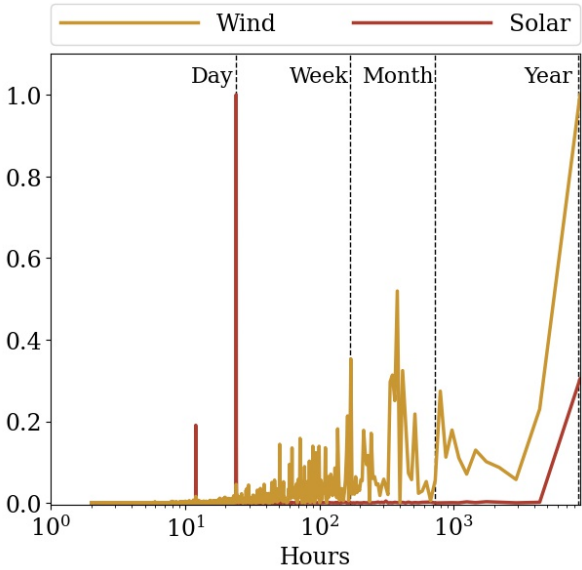


**Figure 26:** Fourier power spectrum for solar PV and wind generation. Solar PV is dominated by the daily frequency, while the annual variation dominates wind generation.

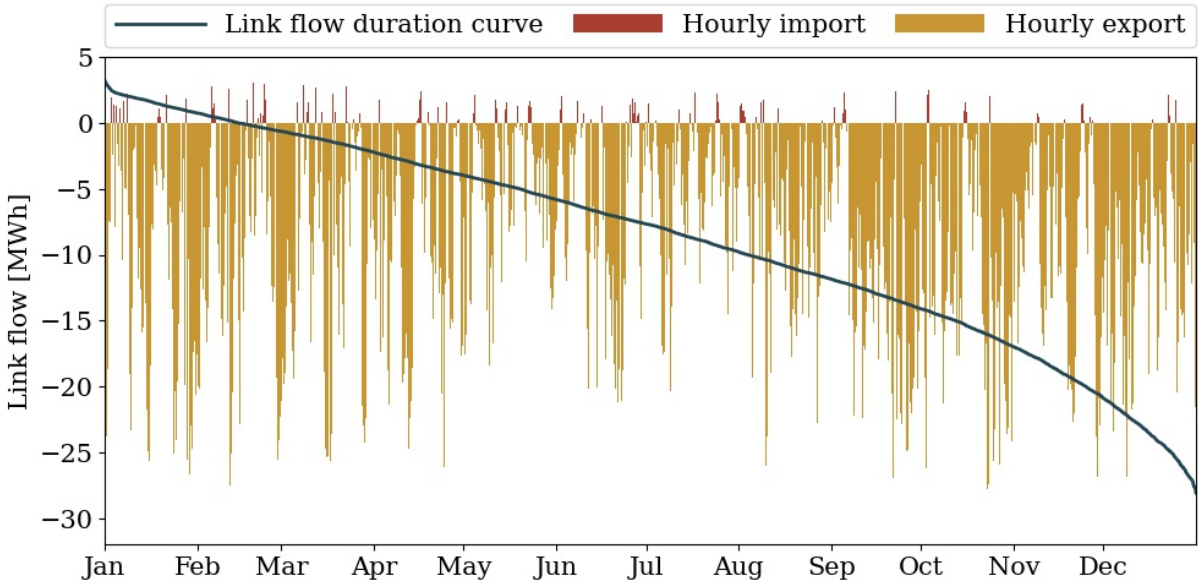


**Figure 29:** As Samsø has a large amount of renewable capacity installed, the export of electricity is far greater than the import, but the import is necessary to meet the electricity demand on Samsø.

#### 4.1.2 Heating

In this section, the electricity and heating sector on Samsø are coupled. This is done by replacing the boilers in the DH sector with heat pumps and resistive heaters, including the individual heating demand supplied by electric heaters, heat pumps, and remaining oil boilers. As Samsø moves towards a fossil-fuel-free future, the remaining oil boilers will have to be replaced, and it is assumed that heat pumps will replace them.

Adding storage in an electrified district heating sector allows the system to increase heat production when the electricity spot price is low or when the spot price makes it undesirable to export the generated electricity to the mainland.

By coupling the electricity and heating sector, the electricity demand profile better matches the annual electricity generation profile dominated by the installed wind capacity. In Fig. 30 the current and coupled electricity demand is compared, and it is clear that the coupled electricity demand doubles in the coldest months of the year.

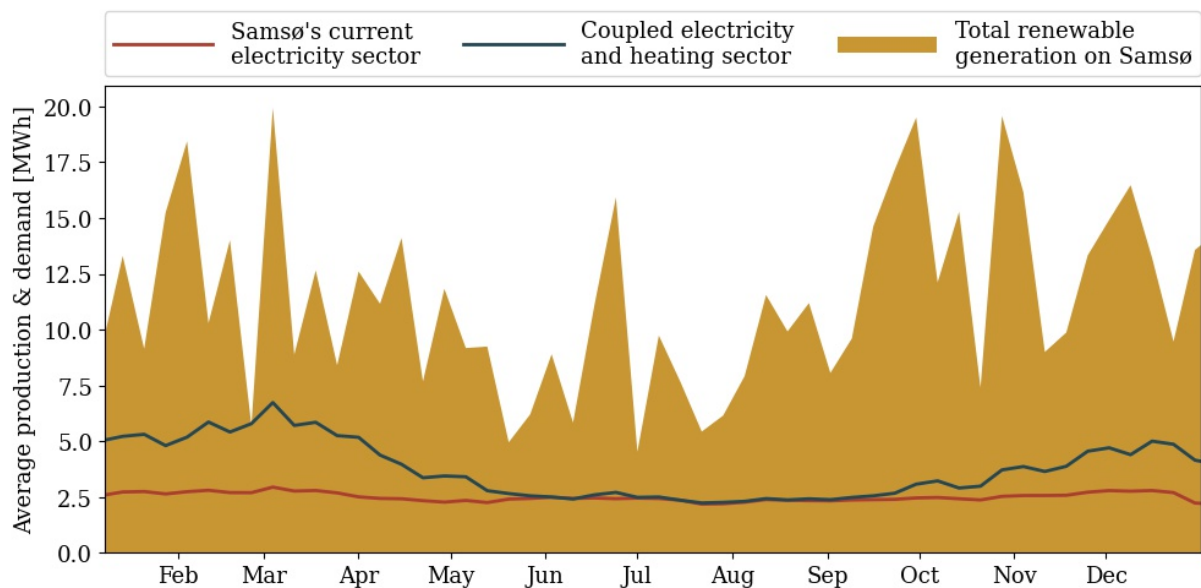


**Figure 30:** Average weekly electricity production and consumption on Samsø. The electricity demand increases when the electricity and heating sectors are coupled, and the electricity demand takes the shape of the heat demand.

As was the case for the district heating plant examined in Chapter 3, heat pumps cover the majority of the heat demand while resistive heaters cover the peak load in the coldest months. When comparing the islands large district heating plant to the smaller ones, it can also be seen that the higher cost for small-scale DH heat pumps causes resistive heaters to cover a more significant portion of the peak load. As the cost of small-scale DH heat pumps is almost 50%

higher than for medium-scale DH plants, it is understandable that the resistive heater capacity is increased, even if it results in higher electricity costs.

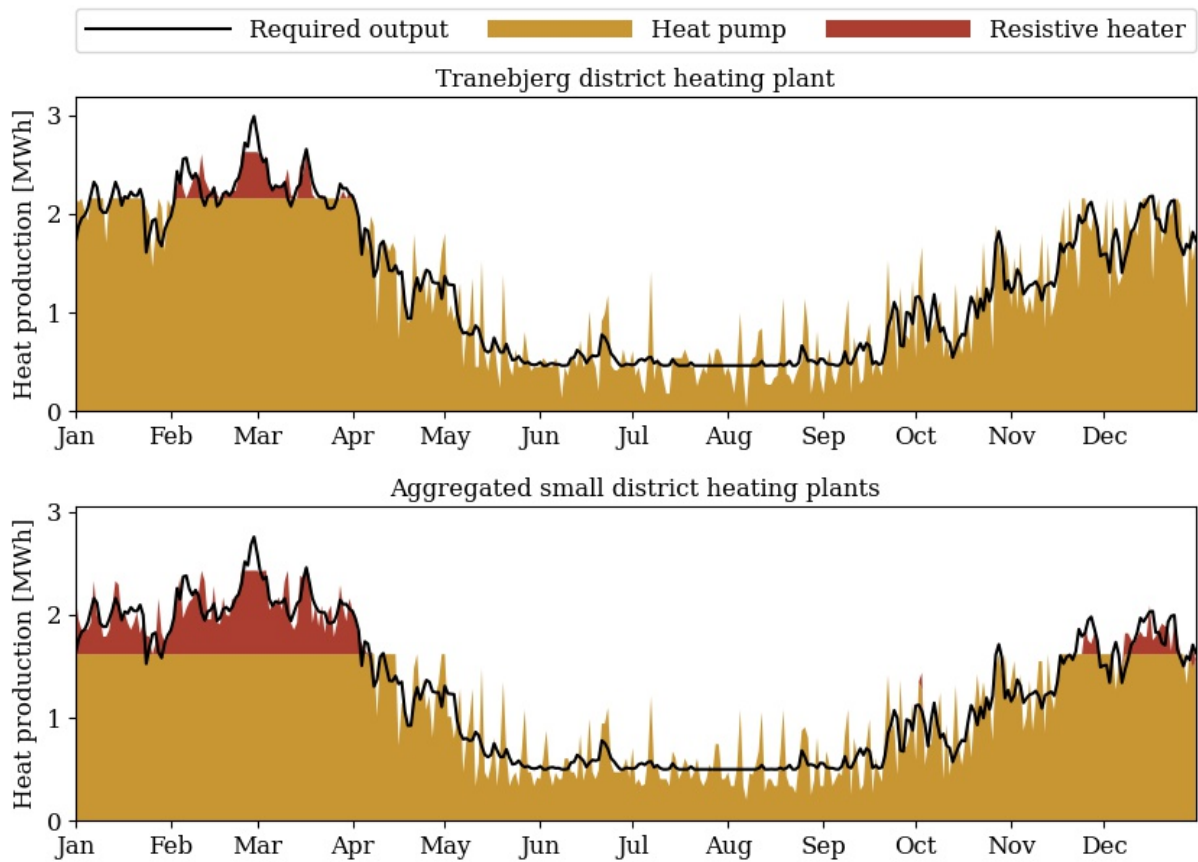


**Figure 31:** Average daily heat production and heat demand for the district heating sector on Samsø. The large plant (top) is modelled separately, while the three small district heating plants are modelled as one aggregated plant.

When the electricity and heating sectors are coupled, the total electricity demand for the island increases. This results in a rise in the annual import, which grows to almost three times that of the current system, as seen in Fig. 32. While this seems like a significant increase, the island still mainly exports electricity, with import only covering 5% of the annual electricity demand for the island.

Coupling the electricity and heating sector lowers the use of the link for export, with an 11% decrease in export in 2018. As wind production and heat demand show a similar annual profile, this coupling notably allows for increased wind capacity without being limited by transmission capacity.

## 4.2 EXPANDING VRES CAPACITIES

### 4.2.1 Electricity and heat

In this section, the installed VRES capacities on Samsø are allowed to expand for a system with coupled electricity and heating sectors. This is examined to determine if the high quality of VRES on Samsø makes it worthwhile to increase the capacities to export more electricity to DK1.

The model is run for the years 2013-2019, and it was only optimal to increase the VRES capacity on Samsø two of those years, as seen in Fig. 33a. For both of these years, only the solar PV is increased. As seen in Fig. 33b these years correspond to a capacity factor slightly higher than average for solar PV. As a year with a marginally higher capacity factor results in a significant increase in solar capacity, solar panels are assumably on the verge of being cost-competitive with the current electricity spot price. With the current associated costs, a capacity factor 5% above the average for Samsø and 20% above the average for Denmark makes them cost-competitive.

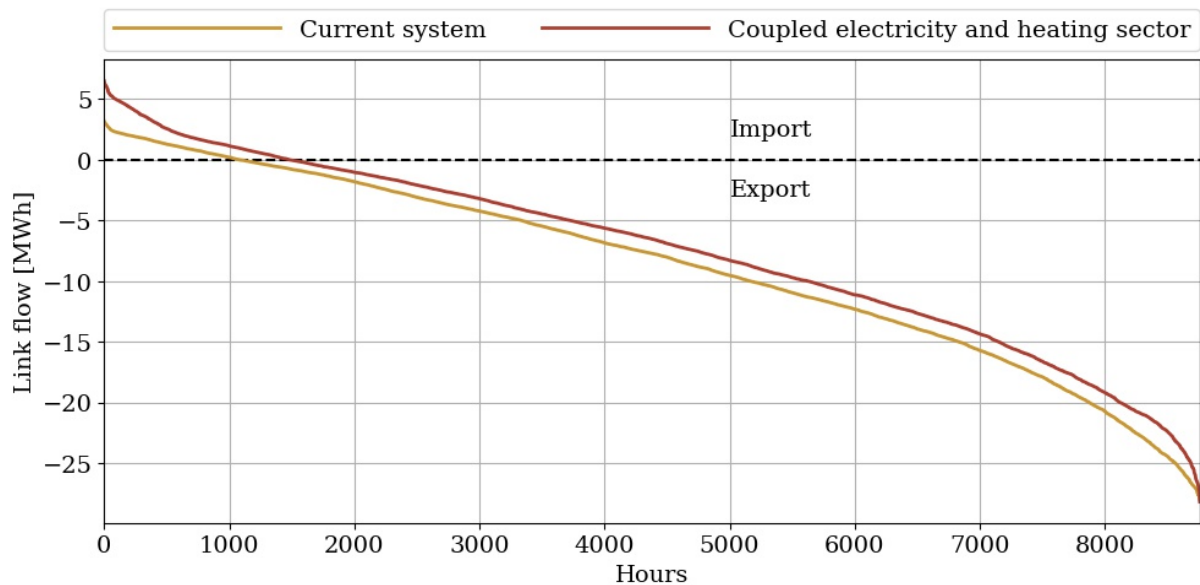


**Figure 32:** Duration curves for the link flow in the current energy system and a coupled electricity and heating sector. The export reduces when the electricity and heat sector are coupled, and in the peak import hours the flow doubles.

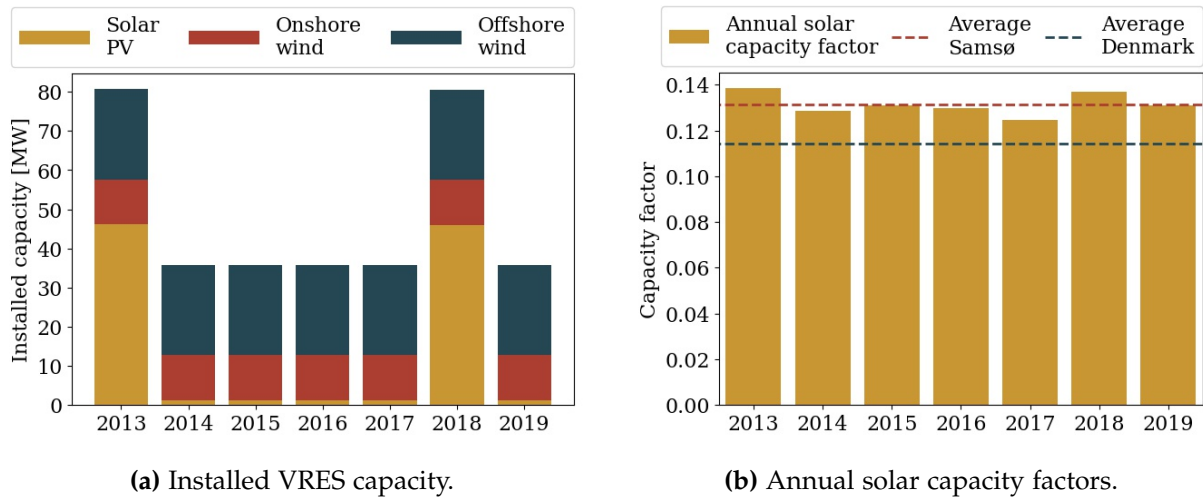


**Figure 33:** Capacities on Samsø for the 7 years modelled. Most years the capacities are not increased, but for two years with a slightly higher capacity factor for solar PV, the installed capacity is increased significantly.

In 2018, where the system installs an extra 45 MW of solar PV, the generation on Samsø occasionally exceeds the demand and export capacity. When this is the case, or when the electricity spot price is negative, electricity generation is curtailed. This can be seen in Fig. 34.

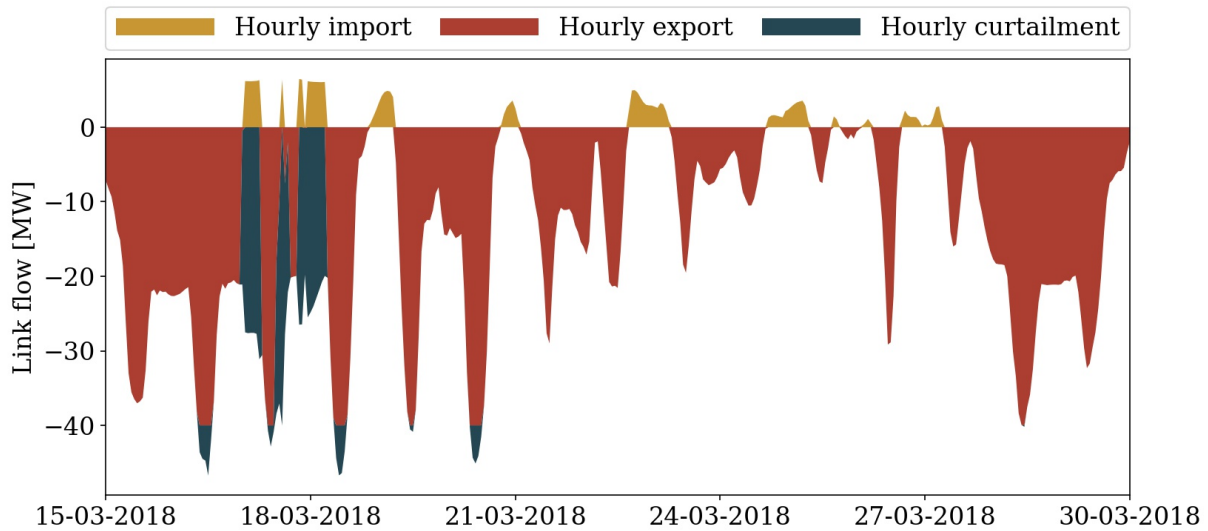


**Figure 34:** The link flow for the optimal capacities for the last half of March in 2018. Electricity is occasionally curtailed due to either link capacity or spotprices.

The curtailed electricity in 2018 was 4258 MWh, which is just below 3% of the annual electricity production in 2018. While this is not much, it is more than twice the necessary import for 2018, as seen in Fig. 35.

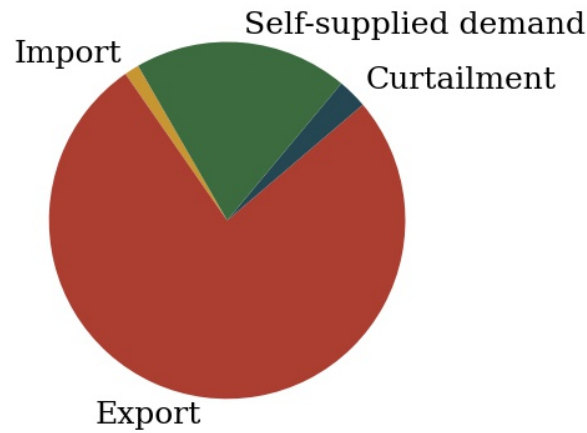


**Figure 35:** Overview of the total electricity generation on Samsø in 2018. Most of the electricity generation on Samsø is exported to DK1, part of it is used to cover the islands electricity demand, and a small part is curtailed.

In Fig. 36 the hourly electricity spot price for 2018 is shown. It is clear that the spot price has a high fluctuation, and it is occasionally below even the modest marginal cost of 3 €/MWh, which is associated with offshore wind. Furthermore, it is frequently below the average annual electricity cost. This, along with the curtailed energy on the island, makes it interesting to examine whether it is beneficial for the system to use storage to balance the generation and spot price fluctuations.

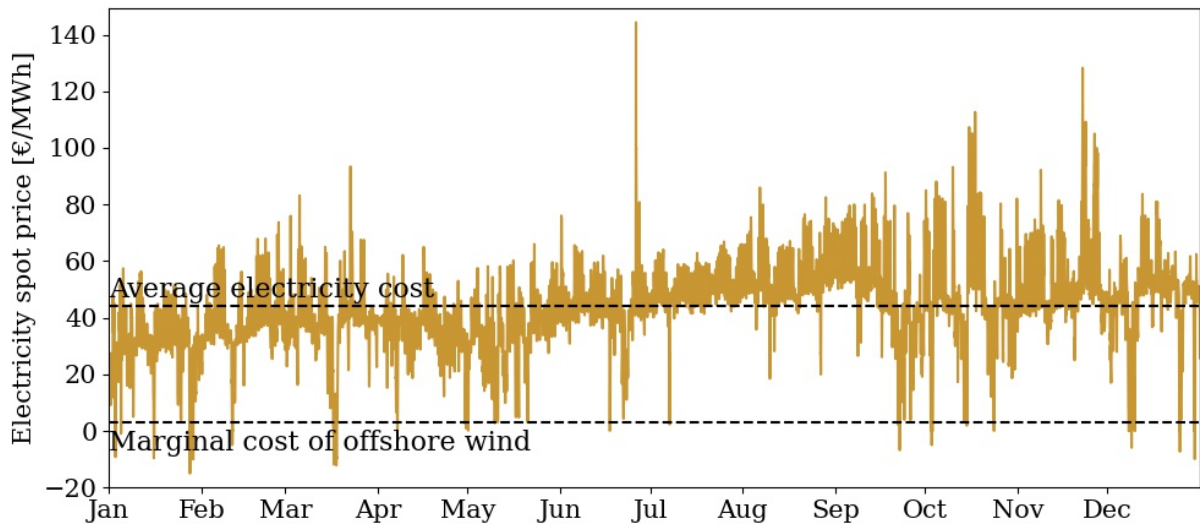


**Figure 36**

## 4.2.2 Hydrogen

Even though hydrogen storage was tested for both the expected reduction in the associated costs towards 2050 and further reduction, no hydrogen storage was included. This shows that no matter the costs, it is hard to compete with the link to DK1, which balances the generation and demand on Samsø. As this link connects to both a constant demand and the option of purchasing electricity from the grid, hydrogen cannot compete, no matter how low the associated costs are, as seen in Fig. 37.

Therefore, the only model where hydrogen was utilised to balance production and demand was a model of Samsø, where the link to DK1 was severed. Without this link, the island was forced to balance production and demand internally, which required a hydrogen storage of 190 MWh.

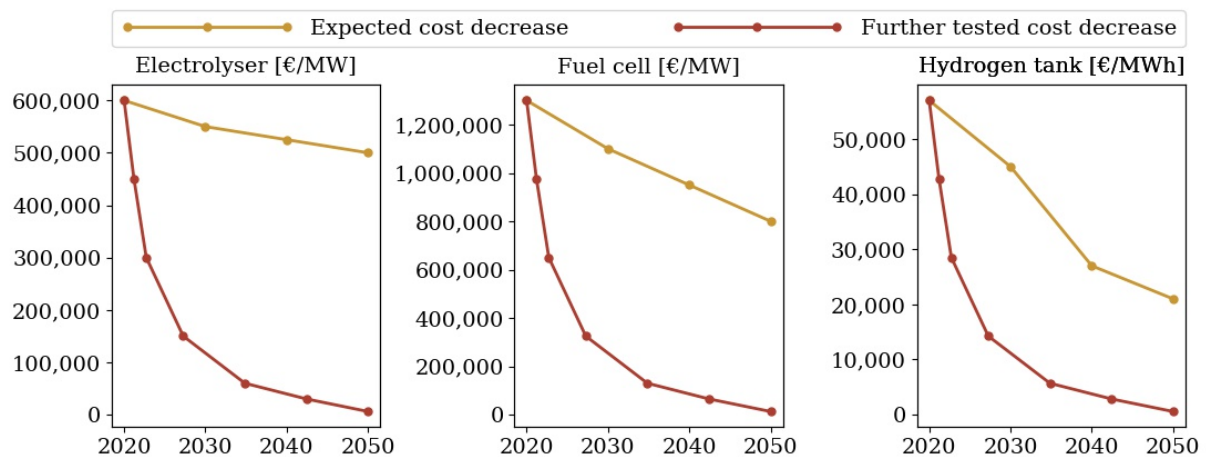


**Figure 37:** Expected cost decrease for hydrogen storage towards 2050. Further increase in associated costs have also been tested.

## 4.2.3 Transport

When the transport sector is coupled to the electricity sector, the electricity demand is increased to cover the demand for transport. However, the system is also given free access to the storage in the BEV's. As a result of coupling the transport and electricity sector, the annual electricity demand on the island increases by an average of 21%. In the two years where solar PV capacity is increased, the capacity is further increased by an average of 3 MW as seen in Table 23.

When looking at the increase in import from the mainland, this exceeds the increase in demand. It follows that the excess must be imported back to the mainland, and this increase in export

**Table 23:** Values for 2018

Description	Electricity demand		Solar PV capacity	
	2013	2018	2013	2018
Value for electricity + heat	32.3 GWh	32,7 GWh	46 MW	46 MW
Value for electricity + heat + transport	39,0 GWh	39,4 GWh	48 MW	50 MW
Increase	20.8%	20.4%	4.5%	9.4%

can be seen in Fig. 39. The reason for this increase in both import and export is found in the systems ability to store and discharge electricity from the transport storage.

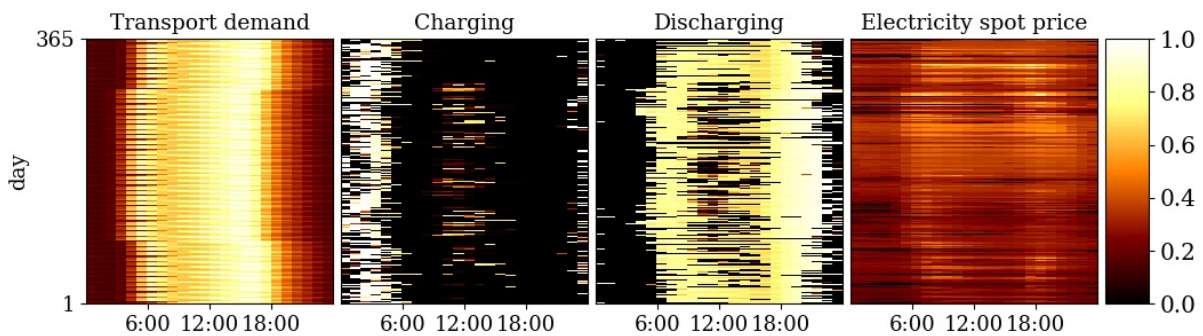


**Figure 38:** Hotmaps for the transport demand, charge and discharge, and electricity spot prices in 2018.

In Fig. 40 the Fourier power spectrum can be seen for the transport demand, the electricity spot price, as well as the charge and discharge of the batteries in the transport sector. Here it is clear that a diurnal frequency almost solely describes the transport demand. This frequency also explains most of the variation for charging the transport storage, but the most significant frequency for the discharge of the transport sector is at 12 hours. The same frequency is significant for the electricity spot price.

To get a closer look at the dynamics of the transport sector, the hourly time-series for these four variables are plotted in Fig. 38. Here it can be seen that the transport demand is highest during the day, with a slight morning peak between 5:00-8:00 and a substantial peak in the afternoon. The transport storage is primarily charged during the night using wind energy. This is due to the constraint ensuring that the filling level is at a minimum of 75% at 5:00. Another slight peak is seen at noon, and since this is almost entirely seen during the summer. This peak is likely due to the peak production of the solar PV at noon.

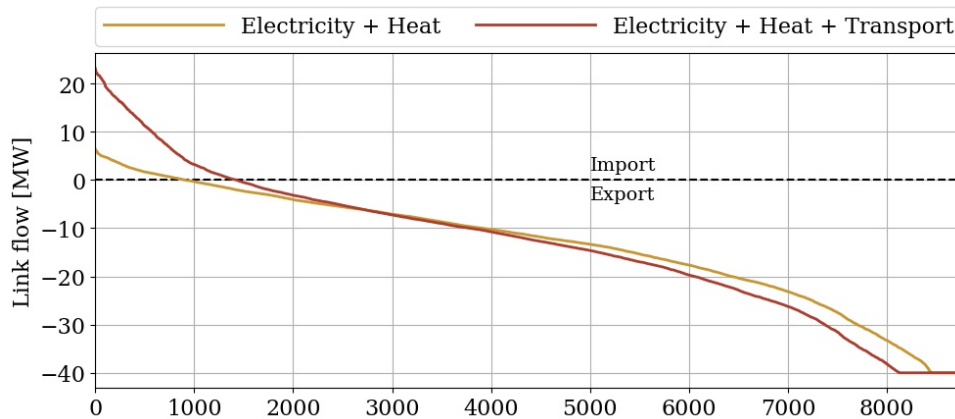


**Figure 39:** Link flow before and after the transport sector is coupled to the electricity sector.

When looking at the discharging patterns, the transport storage is mostly discharged during the peak electricity loads in the morning and evening. These periods are also when there are daily peaks in the electricity spot price.

Even with an increase in load from the transport sector, the system cost decreases by an average of 100,000 € /year, corresponding to 2% of the annual system cost. This decrease in annual costs, along with the increase in both import and export seen in Fig. 39, suggests that the system imports electricity when the spot price is low and sells at a profit during the peak.

The ability to balance production in the transport sectors storage has little impact on the average curtailment. The only significant curtailment reduction achieved by coupling the electricity and transport sector occurs in the years where the installed solar PV is expanded as seen in Fig. 41. These years production is occasionally curtailed due to export limitation, and this curtailment is reduced when the system has access to the transport storage.

The hourly export and curtailment for selected days can be seen in Fig. 42. The plot of hourly export also shows how export peaks at noon every day when solar production is highest, and how it drops after midnight, when the system is forced to charge the BEV, as per the constraint requiring a 75% filling level at 5:00.

#### 4.2.4 Cost reductions

In the coming years, the costs associated with installing and maintaining renewable energy capacity are expected to decrease. In this section, the optimal capacities towards 2050 are determined as a function of the expected cost progression outlined in [1].

The expected capital cost decrease for the different technologies can be seen in Fig. 43. Here solar PV is expected to have the most significant cost decrease, with the cost in 2050 being 40%

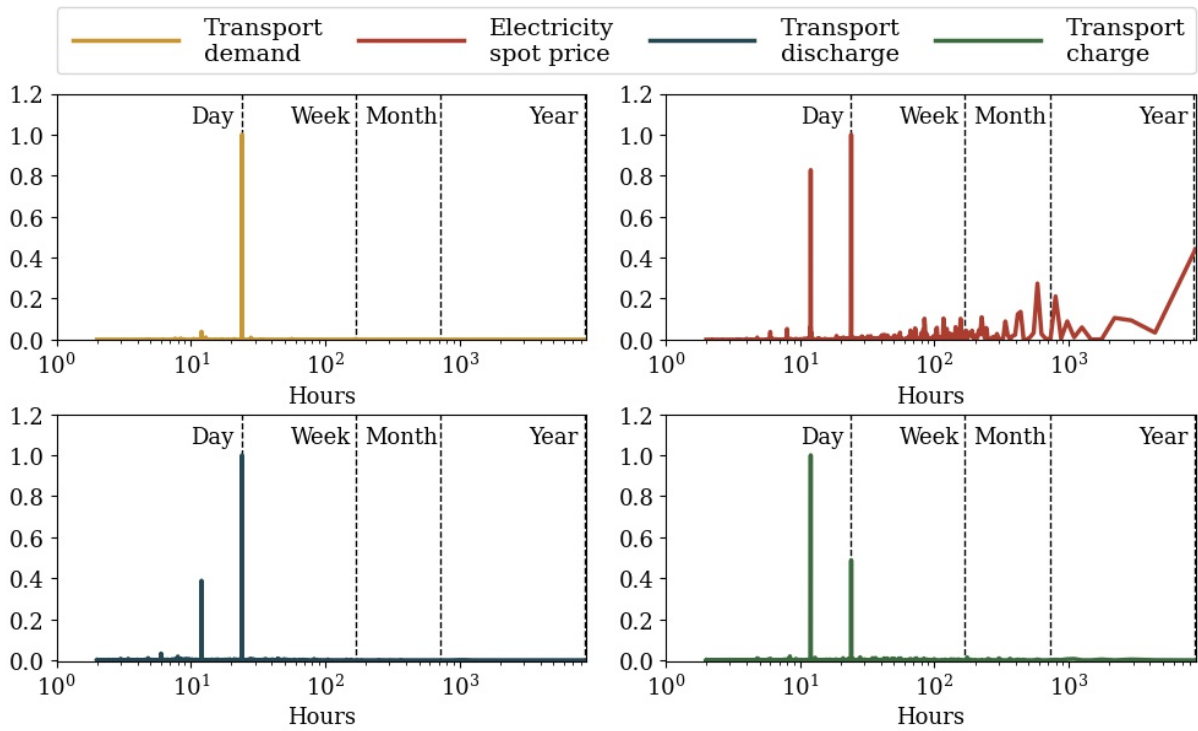


**Figure 40:** Fourier power spectrum for the transport demand, electricity spot price, and transport storage charge and discharge.

lower than the cost today. Both on- and offshore wind seem to plateau at a cost around 15% lower than today.

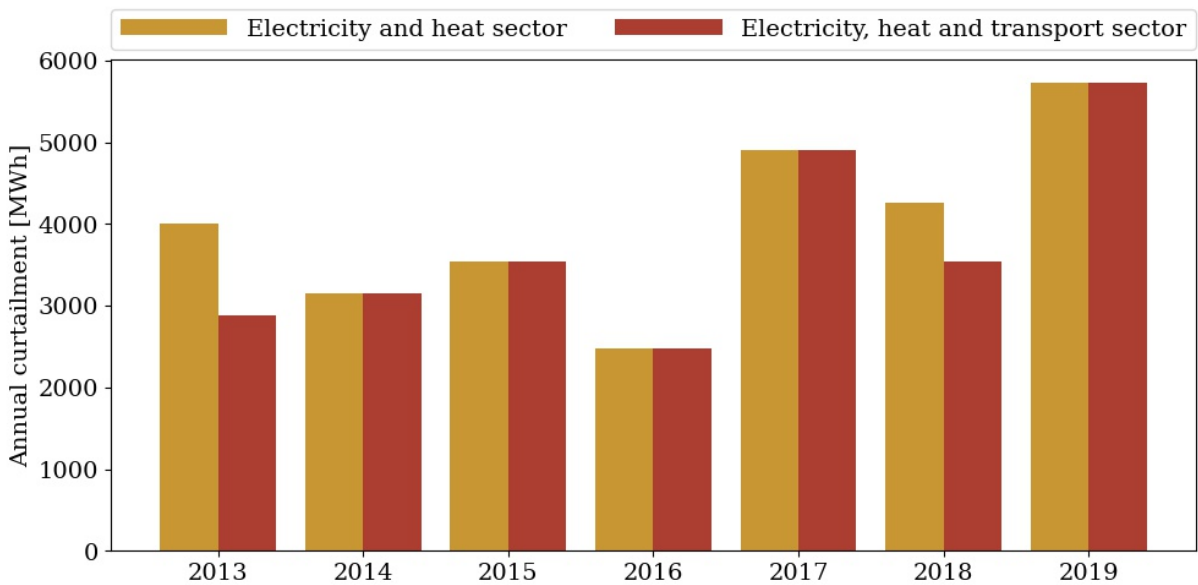


**Figure 41:** Annual curtailment before and after transport sector coupling. Curtailment is only reduced for the years with increased solar capacity.

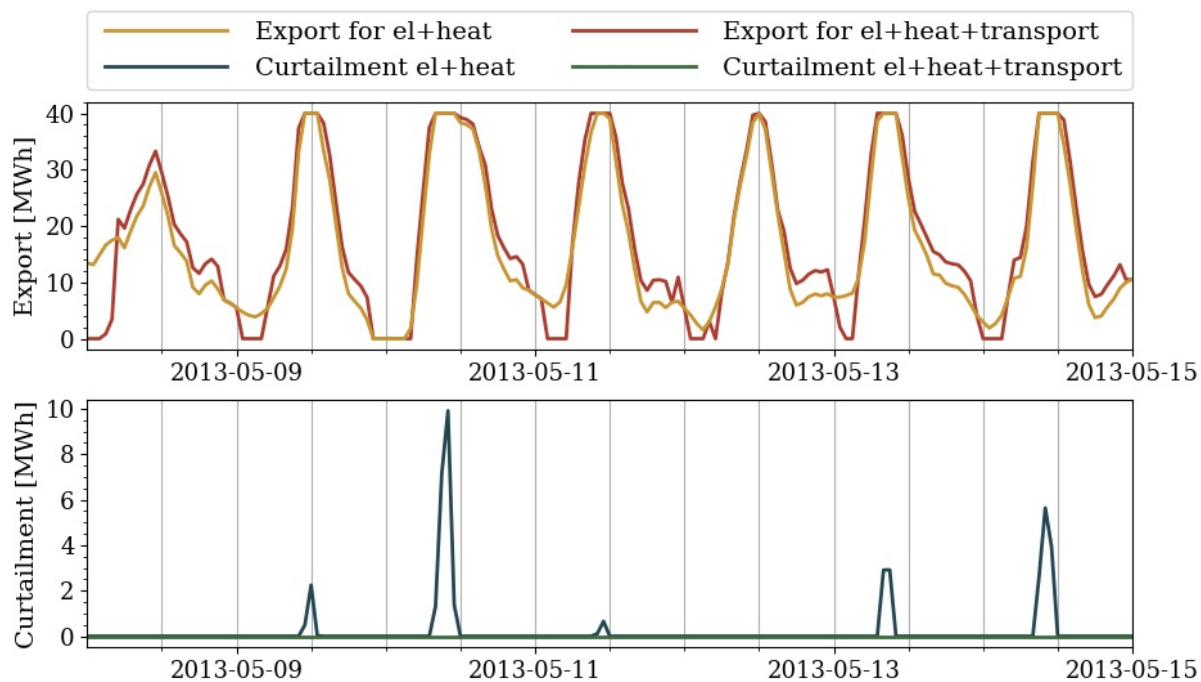


**Figure 42:** Hourly export and curtailment for a selected week in May 2013. Here it can be seen how the reduction in curtailment occurs when electricity is curtailed due to export limitations.

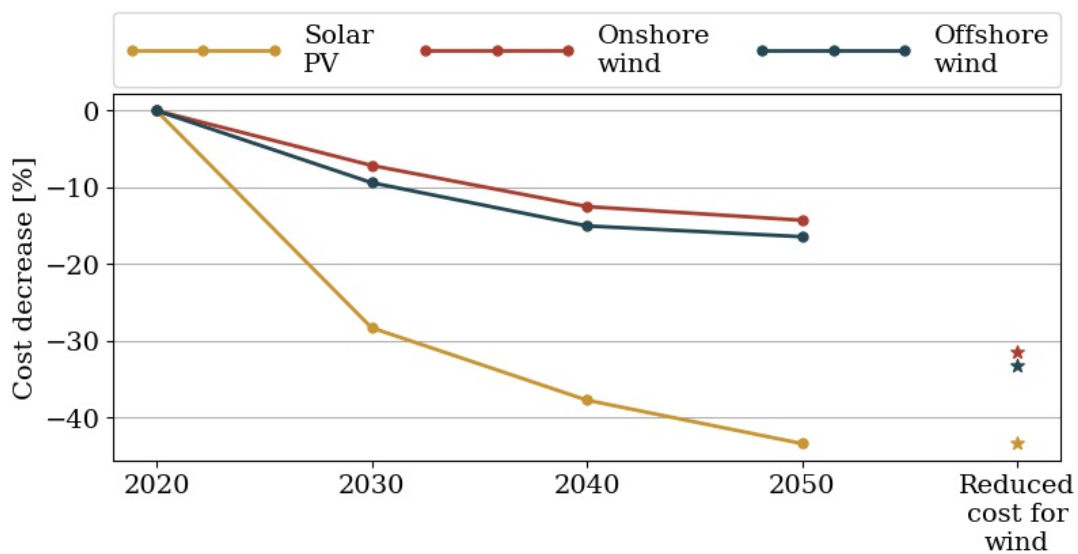


**Figure 43:** Expected cost decrease for the included renewable generation technologies, taken from the Danish Energy Agency (DEA) Technology Database [1] and artificial decrease in wind costs.

As the cost of installation decreases, it is beneficial for the system to increase the installed capacity. However, even with the decrease in associated costs, and the above-average wind capacity factors on Samsø, it is not beneficial for Samsø to increase its wind capacity. Conse-

quently, the increase in renewable capacity on Samsø is limited to solar PV, as the significant decrease in capital cost causes solar PV to outperform wind, both on- and offshore.

It is worth noting that the electricity spot price used in this model reflects the current electricity system in DK1, where CO<sub>2</sub> is emitted. Therefore, a change in the prices in DK1, which will likely come as the electricity sector changes, could make the installation of wind on Samsø competitive with the electricity market.

The optimal capacities for the years 2020-2050 can be seen in Fig. 44. In the first plot, the transmission capacity is limited to the current link. Secondly, the link is allowed to expand, and finally, the capacity limit for solar PV defined in Section 2.3.2 is removed.

With the current link, the optimal solar capacity is limited by transmission capacity by 2040. However, the cost decrease from 2040 to 2050 still allows for an increase of 3 MW, even though this increases curtailment when production exceeds the link capacity. When the link is allowed to expand, the maximum allowed capacity for solar is reached by 2040. Surprisingly, even as this limit is reached, wind installations are not increased beyond the current capacity. As the limit for solar capacity is removed, the installed solar PV skyrockets in 2050 to 265 MW, accentuating both the significant cost decrease expected for solar PV and the high quality of solar irradiation on Samsø, which is 15% higher than the national average.

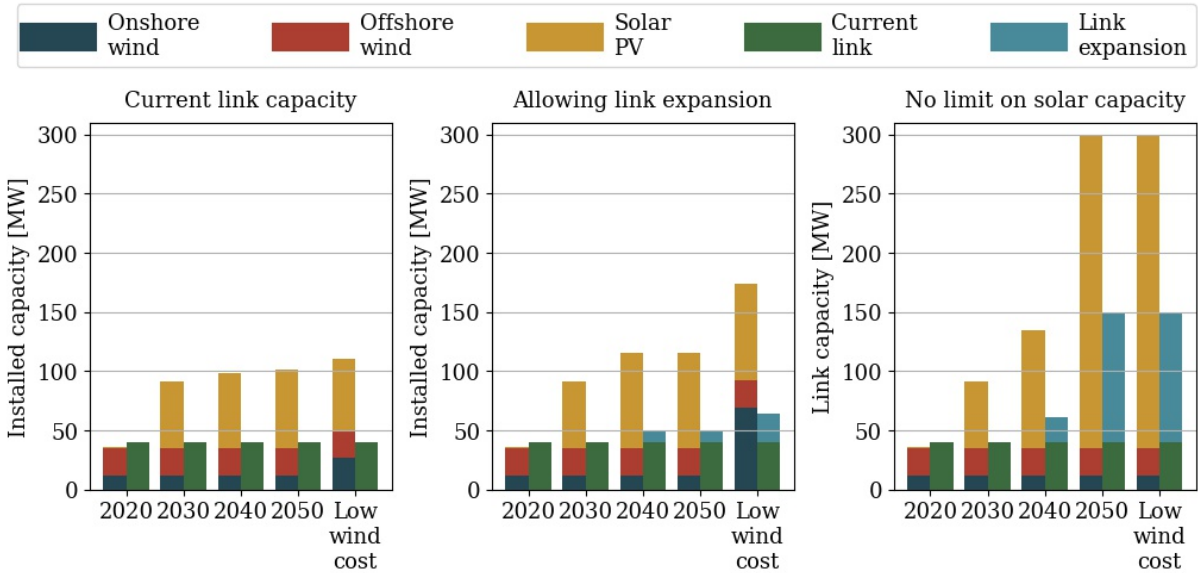


**Figure 44:** Installed capacity for 2020-2050. The optimal capacities are first found for the current link, then the model is allowed to increase the transmission capacity, and finally the constraint for the allowed solar PV capacity is removed.

### 4.3 DISCUSSION

The role of storage technologies throughout the decarbonisation of the European energy system was investigated by Victoria et al. in [22]. In the modelled system for Samsø, CO<sub>2</sub>-emissions were not directly included. However, as this model also investigates an increasingly coupled energy system based on renewable generation, it is still relevant to compare results from the two models.

In [22] it was found that hydrogen played a significant role in balancing generation and demand, as CO<sub>2</sub>-emissions were capped at 5% of the 1990 levels. Here hydrogen storage equivalent to 19.4 hours of average demand was found optimal to balance the system. When including the option of balancing the generation on Samsø with hydrogen, this was not cost-optimal. Even as the associated costs were reduced first to the expected costs in 2050, and then beyond to just 1% of the current costs, no hydrogen storage was included.

The reason for this is that Samsø, unlike the countries modelled in [22], is a small island connected to the mainland. DK1 has a load that is more than 500 times that of the island and more than 35 times what the average generation on Samsø would be for the maximum allowed capacities. This allows the model to treat DK1 as an infinite sink and source of electricity from the grid. As such, any costs associated with hydrogen storage makes it hard for hydrogen to compete.

In [22] it was also found that with an electrified transport sector, able to contribute with vehicle-to-grid services, batteries were unnecessary. Due to this and the link to DK1, it was not relevant to include battery storage in this model.

When the transport sector is electrified, the connected storage is equal to 18.6 hours of average electricity demand, which far exceeds the optimal battery capacity of 1.4 hours found in [22].

The model's preference for installing solar PV, rather than wind, is promising for the plans to construct a solar power plant on the island. Although this is not quite cost-optimal for the current cost given in [1], it will be cost-optimal by 2030. However, the future solar power plant's planned capacity will require significant curtailment due to link capacity. While the modelled system curtails wind before solar, as solar PV has no associated marginal cost, the reality is different. With the current link capacity, electricity from an 80 MW solar power plant will be curtailed unless combined with storage, allowing the electricity to be sold when link capacity is available.

It has not been tested whether storage is worth the investment as the cost of solar panels decreases and the islands capacity increases. While solar production can be stored in the transport sector, this might not be enough to limit curtailment during the summer if an 80 MW solar plant is established without expanding the transmission capacity to DK1.

## 5 CONCLUSION

---

In this thesis, a selected district heating plant on Samsø is examined in detail. The purpose of this examination is to determine whether the reduced electricity levies has made the production cost for heat pumps cost-competitive with the existing biomass burner. It has also been investigated how the plant operates and how sensitive the optimal capacities are to external factors.

Among other factors, the plant has been investigated for annual variations and different heat sources for the heat pump to ensure that the recommended system can accommodate the heat demand in any possible scenario. Furthermore, a cost sensitivity analysis was done to determine how the layout of the plant would change when the associated costs varied within the bounds of uncertainty for each component and the electricity market.

The partial exemption from levies for electricity used for heat production has made the heat production of the electrified plant cost-competitive with the current straw boilers. While the investment costs, especially for the heat pump, are high, continuing with biomass also requires investments to extend the plant's lifetime and reduce smoke pollution.

The plant primarily produces heat with a 0.8 MW air-sourced heat pump and uses a 0.4 MW resistive heater to cover the peak demand in the colder months. These components are almost exclusively operated with an on/off regulation, utilising the 10 MWh storage to cease production when the electricity price is high.

The cost uncertainties of the heat pump and the electricity cost significantly impact the size of the heat pump and the annual system cost. In contrast, the cost variation for the heat storage and resistive heater mainly influence each other. Heat storage has the highest cost uncertainties, with costs ranging from -40% to +170% of the average cost, but the effect on both the heat pump and the system cost is minuscule.

When looking exclusively at heat production costs, the ground-sourced heat pump has the lowest expense with a production cost of 33 €/MWh. Compared to this, both the air-sourced heat pump and the current straw boiler has a production cost of 35 €/MWh. Besides the lower production cost, the ground-sourced heat pump will not result in any noise pollution. However,

the ground-sourced heat pump has an annual system cost 14% higher than the air-sourced heat pump.

Regarding the resistive heater and heat storage, both are very cheap components, which contribute only 2.5% to the annual system cost. Consequently, increasing the capacity of either of these components is an inexpensive way to safeguard the stability of the district heating plant.

The energy system on Samsø has been studied for several historical years to determine the effect of sector coupling in the near-future. Here the electricity sector was first coupled to the heating sector, and next, these two sectors were coupled to the transport sector. The quality and dynamics of VRES on the island were examined, along with the changing demand as sector coupling increased. The role of the link facilitating import and export were investigated to understand its dynamics and how the ratio of import and export changed as the electricity demand on the island increased and the island's renewable capacities were allowed to expand. Furthermore, it was tested if the system would benefit from balancing production and demand with hydrogen storage.

Finally, a model was established to assess the long term decrease of VRES installation costs and the following optimal VRES capacities for Samsø. To ensure that the long term capacities are not based on a singular year, average time series have been generated for all fluctuating data inputs. These hourly averages are calculated from the seven years, which were modelled in the sector-coupled system.

The study of Samsø's energy system unsurprisingly revealed that the island is a net exporter. The quality of VRES on Samsø are above the national average. The average capacity factor for wind is 9% higher, while the solar capacity factor exceeds the average for Denmark by 15%. For the current electricity sector, import makes up less than 2% of the flow through the link to the mainland. When this sector is coupled to the heating sector, the annual profile of the electricity demand better matches the renewable production on Samsø. This production comes primarily from wind, which generates more electricity in the winter than in the summer. The same season where the demand for space heating emerges. When the heat and electricity sector are coupled, more electricity is used on the island. Subsequently, the export is reduced by 11%. Additionally, the import increases significantly to almost three times that of the current system.

When the renewable capacities on Samsø are allowed to increase, the installed wind and solar remain at their current levels most years. However, two years out of the modelled seven results in an increase in solar PV, as the solar capacity factor is higher than average for these two years. These years the installed solar PV increases from 1.3 MW to 46 MW.

Coupling the transport sector to the electricity sector allows the system access to the storage capacity in the BEV's. The storage is mainly used to import electricity from the mainland when the electricity spot price is low and export it back at a profit after the spot price has increased. The transport storage is primarily charged during the night, supplemented around noon during the summer months, where solar production peaks. The discharge occurs during the morning and evening peaks of electricity demand and spot price. This dynamic results in a reduction in system cost of 2%, even with an increase in electricity demand of 21%.

Access to storage in the transport sector only reduces the curtailment for the years with increased solar capacity. As these years are the only years where production can exceed the transmission capacity, the reduction in curtailment does not occur when electricity prices are low but rather when electricity is curtailed due to export limitations.

Hydrogen can play a considerable role in the future by balancing fluctuating VRES. Nevertheless, it is not beneficial for Samsø to install hydrogen storage in this model, even at a fraction of the current installation cost. This is due to the way the system is modelled. When Samsø is coupled to a constant demand in DK1 and has the option of purchasing electricity from the grid, DK1 essentially acts as an infinite sink and source. Consequently, any associated costs make it hard for hydrogen to compete.

If Samsø wishes to expand its renewable capacities, solar PV is the best way to go. Currently, the costs are on the verge of being cost-competitive with the electricity spot price. However, with the projected decrease in installation costs, an average year on Samsø warrants an increase by 2030.

If the transmission capacity increases, Samsø will benefit from installing the maximum allowed solar PV by 2040. Nevertheless, even after this constraint is activated, and the installation costs for all VRES decrease further in 2050, the installed wind capacity is not increased.

The predicted cost decrease for wind appears to plateau at a cost around 15% below the current cost, and the modelled system only increases wind capacity for a cost decrease of more than 30%. Despite this considerable artificial cost decrease, onshore wind capacity is only expanded when the link is allowed to expand, and the allowed solar PV is capped at 81 MW. When the constraint limiting solar PV is removed, the previously included onshore wind is discarded to increase the solar PV.

If the time frame for the project had allowed it, it would have been interesting to test the optimal heating system for Samsø. This would be done by combining the island's heat demands into a singular demand and allowing the system to select between individual, small- and medium-scale district heating plants. The capital cost for individual heat pumps lies between the costs

of small- and medium-scale heat pumps for district heating, and while the district heating plants allow for heat storage, they also come with significant heat losses in the grid. For that reason, it would be interesting to examine if the small district heating plants on Samsø are cost-optimal and if the significant grid losses in all the district heating plants cause the system to install individual heat pumps instead.

Additional time would also have given the board of Ballen-Brundby district heating plant time to conclude the cost of lifetime extension for the current straw boiler. However, as these costs are unknown, it cannot be finally concluded if the system costs of the electrified district heating plant can compete with biomass, even if the production costs can.

Finally, considering the energy system on Samsø, additional research into the projected future electricity cost could help ensure the model's accuracy for the future energy system on Samsø. Other factors that could cause an expansion of Samsø's future renewable capacity are government grants to advance renewable installations or the establishment of carbon taxes.

## BIBLIOGRAPHY

---

- [1] Danish Energy Agency. Technology - renewable fuels (2017)
- [2] Statbank denmark. URL <https://www.statbank.dk/statbank5a/default.asp?w=1536>. [Online; accessed October 30th, 2020]
- [3] P.G. Wang, M. Scharling, K.B. Wittchen, C. Kern-Hansen, 2001–2010 dansk design reference year supplerende datasæt: Projektrapport til energistyrelsen: Data til teknisk dimensionering for parametrene atmosfæretryk, vindretning, skydække, vandtemperatur og jordtemperatur samt data til byggesagsbehandling (2013)
- [4] P.A. Østergaard, J. Jantzen, H.M. Marczinkowski, M. Kristensen, Business and socio-economic assessment of introducing heat pumps with heat storage in small-scale district heating systems, *Renewable energy* **139**, 904 (2019)
- [5] Danish Energy Agency. Technology data - technology catalogue for individual heating (2016)
- [6] Danish Energy Agency. Technology data - energy storage (2018)
- [7] J. Jantzen. Personal communication
- [8] Danish Energy Agency. Technology data - generation of electricity and district heating (2016)
- [9] Renewables ninja. URL <https://www.renewables.ninja/>. [Online; accessed September 30th, 2020]
- [10] Responsible island 2019. URL <https://energiakademiet.dk/oe-prisen-responsible-island-2019-gives-til-energiakademiet-paa-samsoe/>. [Online; accessed May 19th, 2021]
- [11] K. Sperling, How does a pioneer community energy project succeed in practice? the case of the samsø renewable energy island, *Renewable and Sustainable Energy Reviews* **71**, 884 (2017)

- [12] Climate action plan - samsø. URL <https://www.samsoe.dk/kommunen/nyheder-og-hoeringer/nyhedsarkiv-2019/ny-klimahandleplan-vedtaget-paa-samsoe>. [Online; accessed May 19th, 2021]
- [13] Ingeniøren - samsø-færgen skal sejle på flydende naturgas. URL <https://ing.dk/artikel/samsoe-faergen-skal-sejle-paa-flydende-naturgas-160178>. [Online; accessed May 25th, 2021]
- [14] Tv2 Østjylland - stor debat om biogasanlæg på samsø. URL <https://www.tv2ostjylland.dk/kommunalvalg/stor-debat-om-biogasanlaeg-pa-samsø>. [Online; accessed May 27th, 2021]
- [15] Energy audit - central denmark region. URL <https://www.rm.dk/om-os/aktuelt/nyheder/nyheder-2019/februar-19/sa-gronne-er-kommunerne/>. [Online; accessed May 19th, 2021]
- [16] Lavere elvarmeafgift er trådt i kraft. URL <https://www.danskenergi.dk/nyheder/lavere-elvarmeafgift-er-traadt-kraft>. [Online; accessed May 19th, 2021]
- [17] J. Jantzen. Decision support for a renewable energy community. URL <http://inference.dk/tiki/tiki-index.php?page=District+heating+efficiency&structure=auto>. [Online; accessed August 15th, 2020]
- [18] Nordpool - historical market data. URL <https://www.nordpoolgroup.com/historical-market-data/>. [Online; accessed November 27th, 2020]
- [19]
- [20] Solar pv project proposal. URL [https://dokument.plandata.dk/20\\_10268990\\_1601889153167.pdf](https://dokument.plandata.dk/20_10268990_1601889153167.pdf). [Online; accessed May 6th, 2021]
- [21] Danish Energy Agency. Technology data - energy transport (2017)
- [22] M. Victoria, K. Zhu, T. Brown, G.B. Andresen, M. Greiner, Early decarbonisation of the european energy system pays off, arXiv preprint arXiv:2004.11009 (2020)
- [23] M. Victoria. Personal communication
- [24] Heat pump minimum outside temperature. URL <https://www.renewableenergyhub.co.uk/main/heat-pumps-information/heat-pump-minimum-outside-temperature/>. [Online; accessed February 11th, 2021]
- [25] H. Christiansen, O. Baescu, The danish national travel survey-annual statistical report 2019 (2020)

- [26] Center for politiske studier - danskerne har færre biler pr. indbygger end i litauen og tjekkiet. URL <https://cepos.dk/abcepos-artikler/0189-danskerne-har-faerre-biler-pr-indbygger-end-i-litauen-og-tjekkiet/>. [Online; accessed May 12th, 2021]
- [27] A.B. Lauritsen, A.B. Eriksen, *Termodynamik, Teoretisk grundlag - Praktisk anvendelse*, 3rd edn. (Nyt Teknisk Forlag, 2000)
- [28] Danish energy agency: Overview of the energy sector. URL <https://ens.dk/en/our-services/statistics-data-key-figures-and-energy-maps/overview-energy-sector>. [Online; accessed April 16th, 2021]

# Appendices

## A INDIVIDUAL HEAT DEMAND

---

The heat demand for the Samsø energy system is split into three categories: Tranebjerg DH plant, the aggregated smaller DH plants, and individual heat demand. In the DH demands, the heat demand is set as the required heat production, as some heat is lost in the grid. The individual heat demand consists of current heat pumps, as well as existing electric heating and oil boilers which are assumed to be upgraded in the future, the sum of these amount to 30% of the total heat demand on Samsø [4].

The total heat demand on Samsø is calculated from the DH production, which [4] has determined to cover 35% of the heat demand of the island. The total heat demand is calculated in Eq. (19)

$$\text{Total heat demand} = \frac{(3.60 + 1.50 + 9.50 + 4.00) \text{ GWh}}{0.35} = 53.1 \text{ GWh} \quad (19)$$

$$\text{Individual heat demand} = \text{Total heat demand} \cdot 0.30 = 15.9 \text{ GWh} \quad (20)$$

While the connected households of the district heating grid were all assumed to be year-round houses, it is assumed that the individual heat demand, covering 30% of the island, covers 30% of the permanent households on the island as well as 30% of the vacation homes. The vacation homes are assumed to be used 10% of the time evenly split throughout the year. The equivalent households covered by the individual heat demand are calculated in Eq. (21), where the number of households is taken from Table 1.

$$\text{Individual households} = 0.3 \cdot (1977 + 1682 \cdot 0.1) = 644 \text{ households} \quad (21)$$

## A.1 HEAT PUMP COP

The Carnot efficiency is calculated as in Eq. (22) where  $T_H$  is the temperature of the hot reservoir, and  $T_C$  is the temperature of the cold reservoir. For the individual heat pumps described in [5] the cold and hot temperature is set to  $-7^\circ\text{C}$  and  $55^\circ\text{C}$ , respectively.

$$\eta_{carnot} = \frac{T_H}{T_H - T_C} = \frac{328 \text{ K}}{328 \text{ K} - 266 \text{ K}} = 5.29 \quad (22)$$

The Carnot efficiency describes the maximum theoretical efficiency of a heat engine, so the real-life process will not have a COP of 5.29, but instead have a COP between 50-80% of the Carnot efficiency [27]. Here the COP is set to 65% of the Carnot efficiency, Resulting in a COP of 3.44 for an outside temperature of  $-7^\circ\text{C}$ .

$$COP_{real} = 5.29 \cdot 0.65 = 3.44 \quad (23)$$

The COP used for the individual heat pumps is calculated from the outside temperature for every hour of the year in the same manner as here.

# B SCALING OF TIME SERIES DATA

---

In this chapter, the scaling factor for on- and offshore wind capacity factors and electricity demands are found.

## B.1 WIND CAPACITY FACTORS

As the geographical resolution of the wind capacity factors from [9] is not able to capture the island of Samsø, and therefore the difference between the on- and offshore wind turbines, the capacity factors for each year are scaled to match the total annual historical production of on- and offshore wind turbines, which have been published by the Danish Energy Agency in [28]. The resulting factors can be seen in Table 24 and Table 25.

**Table 24:** The onshore production is on average 40% higher than the historic production, when using the capacity factors taken from [9] directly.

	Year	2013	2014	2015	2016	2017	2018	2019
Modelled onshore production		36,847	38,638	42,080	36,386	39,976	36,134	38,851
Historic onshore production		27,066	28,791	30,829	26,104	28,946	24,519	26,772
Onshore scaling factor		0.73	0.75	0.73	0.72	0.72	0.68	0.69

**Table 25:** The modelled offshore production matches the historic production better than the onshore production, suggesting that the island of Samsø is not captured in the model generating the capacity factors.

	Year	2013	2014	2015	2016	2017	2018	2019
Modelled offshore production		77,419	81,359	88,477	76,481	84,194	75,949	81,724
Historic offshore production		77,622	79,608	85,375	67,389	80,591	75,628	82,113
Offshore scaling factor		1.00	0.98	0.96	0.88	0.96	1.00	1.00

## B.2 ELECTRICITY DEMANDS

The electricity demand for Samsø is calculated for two different scenarios, the current energy system and a coupled electricity and heating sector.

### B.2.1 Current system

The average annual electricity demand for Samsø, given in [4], is 21.5 GWh, and this is used to scale the hourly electricity demand in DK1 for 2013-2019, published by [18]. The scaling factor,  $f$ , is found by dividing the electricity demand for Samsø with the total electricity demand in DK1 from 2013-2019.

$$f = \frac{21.5 \text{ GWh} \cdot 7 \text{ years}}{139,042 \text{ GWh}} = 1.08 \cdot 10^{-3} \quad (24)$$

### B.2.2 Coupled electricity and heating sector

As the individual heat demand is included separately in the coupled system, the electricity used for this heat production must be removed from the annual electricity demand before the latter is used to scale the hourly electricity demand of DK1 to the demand on Samsø.

[4] states that 5% of the islands annual heat demand of 53.1 GWh is covered by electric heating, and 6% by heat pumps. Assuming an efficiency for electric heating of 0.99, and a COP for individual heat pumps of 3.44, as found in Appendix A, the annual electricity used for heating on Samsø is calculated in Eq. (25).

$$\text{Electricity for heating} = \frac{0.05 \cdot 53.1 \text{ GWh}}{0.99} + \frac{0.06 \cdot 53.1 \text{ GWh}}{3.44} = 3.61 \text{ GWh} \quad (25)$$

The electricity used for heating is then subtracted from the current annual electricity demand, as this is now modelled separately.

$$\text{Annual electricity demand} = 21.5 \text{ GWh} - 3.61 \text{ GWh} = 17,9 \text{ GWh} \quad (26)$$

The annual electricity demand for the island, when the electricity and heating sectors are coupled, is then reduced from 21.5 GWh to 17.9 GWh, and the hourly electricity demand in DK1 is instead multiplied by  $0.901 \cdot 10^{-3}$ , as calculated in Eq. (27)

$$f = \frac{17.9 \text{ GWh} \cdot 7 \text{ years}}{139,042 \text{ GWh}} = 0.901 \cdot 10^{-3} \quad (27)$$

# C MODEL OVERVIEWS

In the model overview all elements that are optimised in PyPSA are marked in bold, the remaining capacities are fixed or irrelevant, as is the case with the electricity grid, where electricity is purchased at an hourly price.

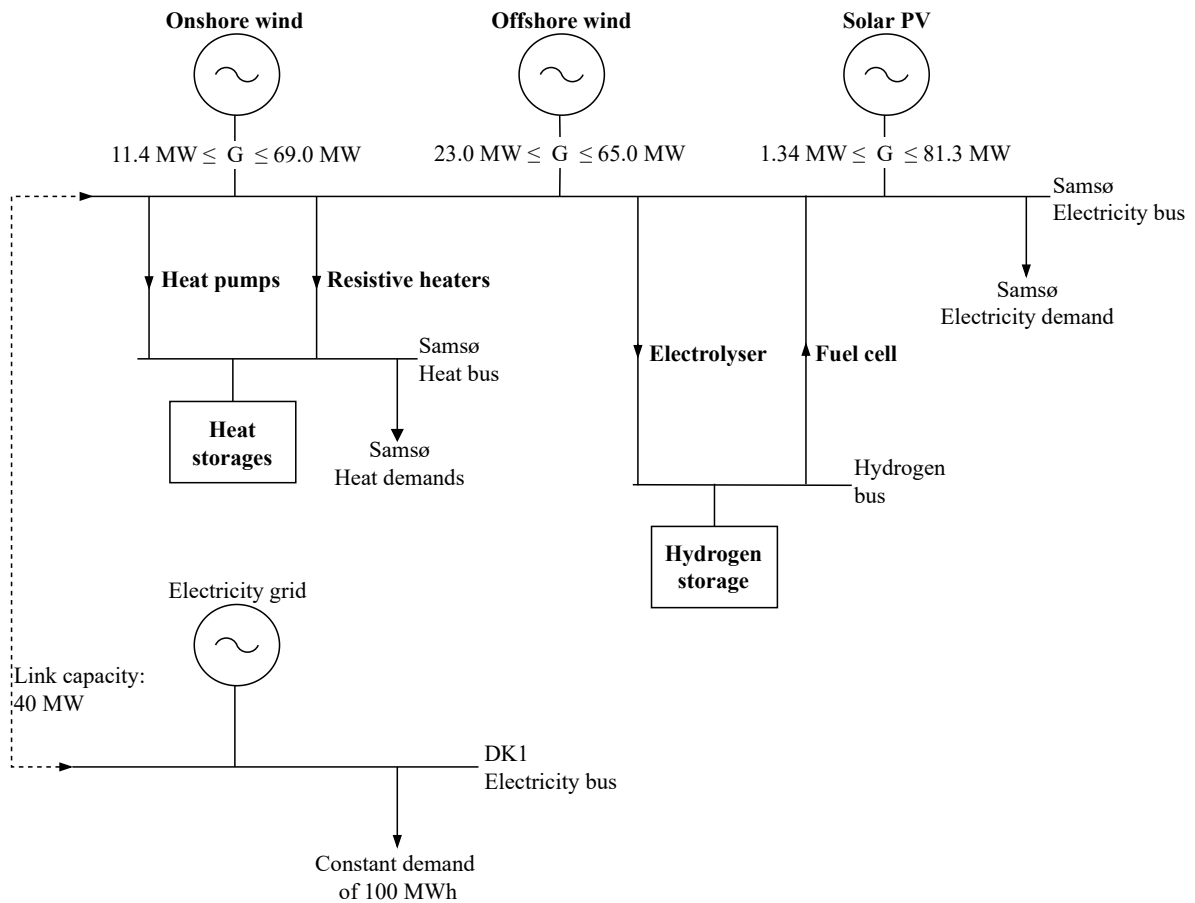


**Figure 45:** Detailed overview of the model for the coupled electricity and heating sector on Samsø with the possibility of hydrogen storage.

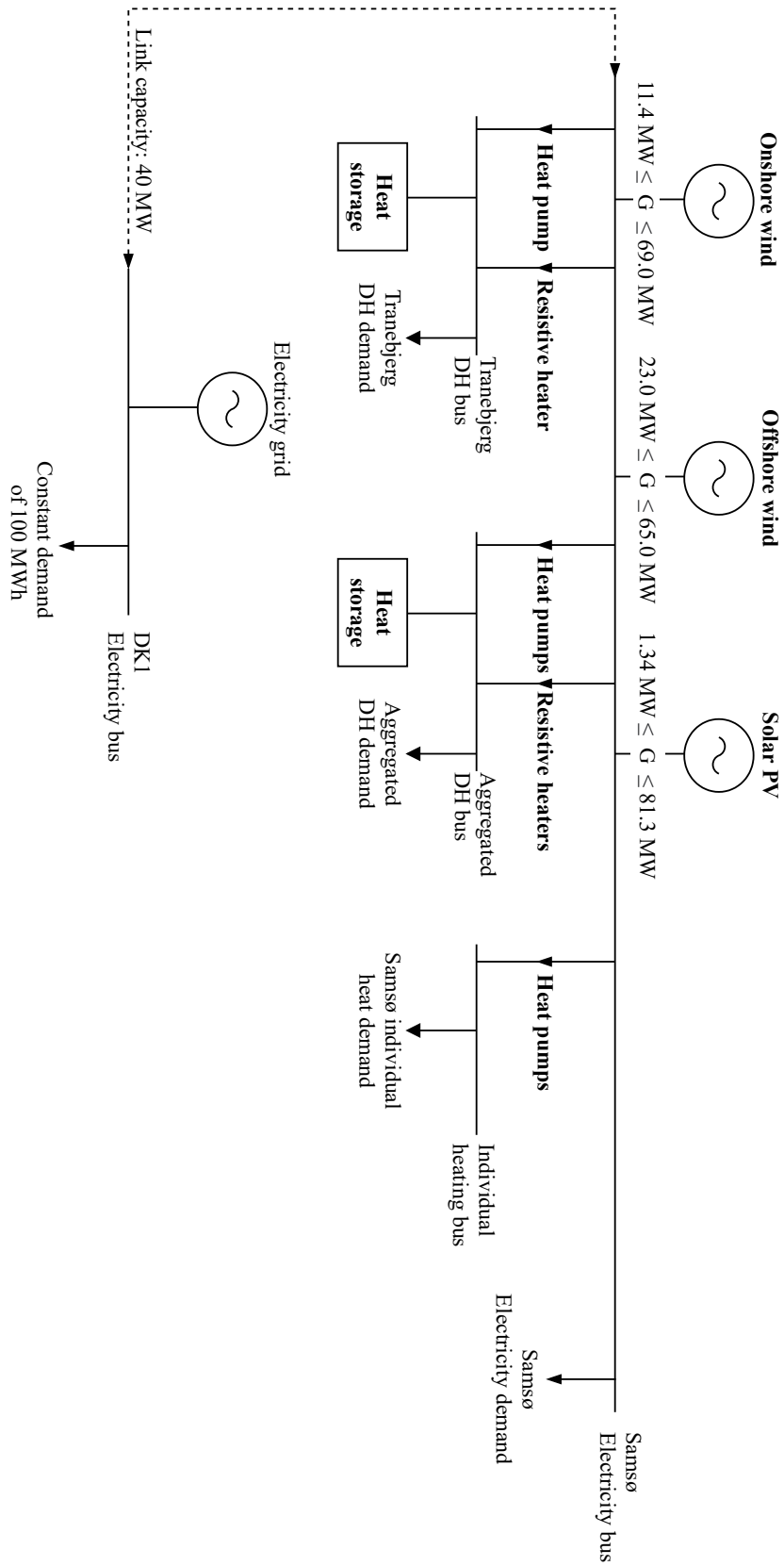


**Figure 46:** Detailed overview of the model for the coupled electricity and heating sector on Samsø.

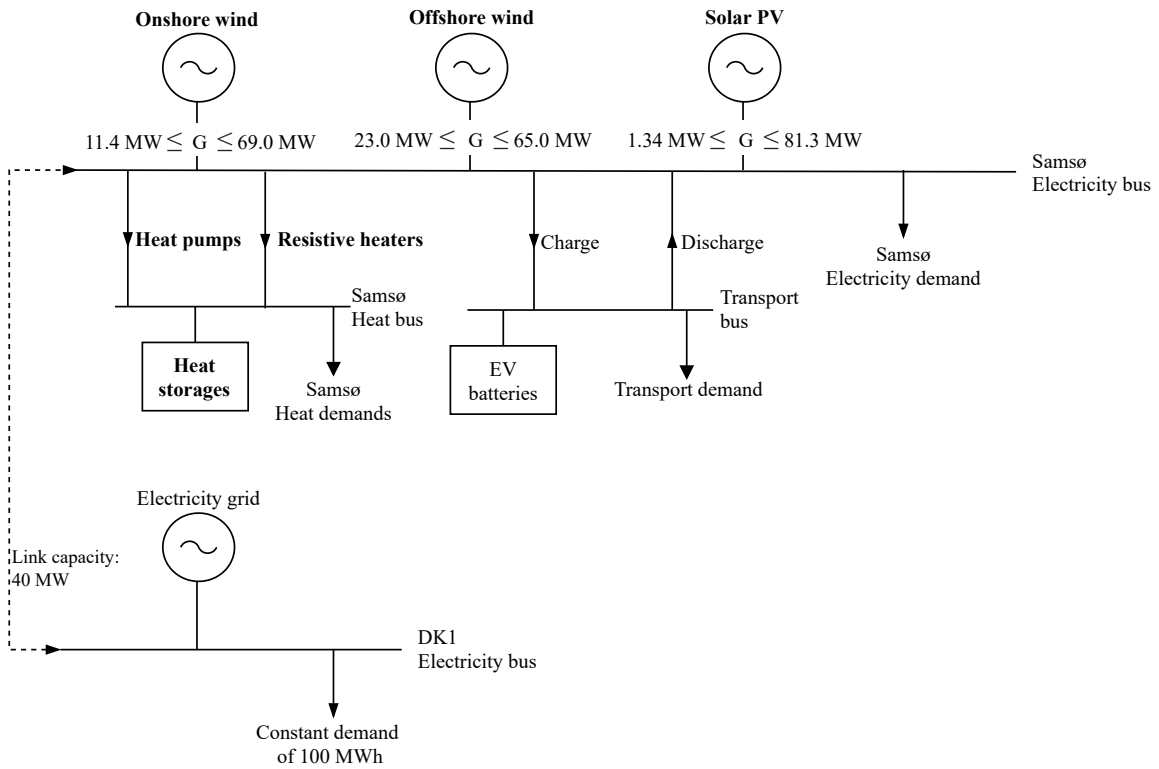


**Figure 47:** Detailed overview of the model for the coupled electricity, heating, and transport sector on Samsø with the possibility of hydrogen storage.